



HAL
open science

Spike detection for calcium activity

Hermine Biermé, Camille Constant, Anne Duittoz, Christine Georgelin

► **To cite this version:**

Hermine Biermé, Camille Constant, Anne Duittoz, Christine Georgelin. Spike detection for calcium activity. 2020. hal-02370401v2

HAL Id: hal-02370401

<https://hal.science/hal-02370401v2>

Preprint submitted on 5 Jun 2020 (v2), last revised 8 Dec 2022 (v3)

HAL is a multi-disciplinary open access archive for the deposit and dissemination of scientific research documents, whether they are published or not. The documents may come from teaching and research institutions in France or abroad, or from public or private research centers.

L'archive ouverte pluridisciplinaire **HAL**, est destinée au dépôt et à la diffusion de documents scientifiques de niveau recherche, publiés ou non, émanant des établissements d'enseignement et de recherche français ou étrangers, des laboratoires publics ou privés.

SPIKE DETECTION FOR CALCIUM ACTIVITY

HERMINE BIERMÉ, CAMILLE CONSTANT, ANNE DUITTOZ, AND CHRISTINE GEORGELIN

ABSTRACT. We present in this paper a global methodology for the spike detection in a biological context of fluorescence recording of GnRH-neurons calcium activity. For this purpose we first propose a simple stochastic model that could mimic experimental time series by considering an autoregressive AR(1) process with a linear trend and specific innovations involving spiking times. Estimators of parameters with asymptotic normality are established and used to set up a statistical test on estimated innovations in order to detect spikes. We compare several procedures and illustrate on biological data the performance of our procedure.

Keywords: Autoregressive process, time series, peaks detection, neuronal activity.

2010 Mathematics Subject Classification. Primary: 62M10, 62F12, 62F03, ; Secondary: 92B25

1. INTRODUCTION

The neurohormone gonadotropin-releasing hormone (GnRH) controls the reproductive function in males and females mammals. GnRH controls the secretion of two pituitary hormones: luteinizing hormone (LH) and follicle stimulating hormone (FSH) that control the secretion of sexual hormones by gonads (estrogens, progesterone from ovary and androgens from testis) and gametogenesis (follicle development and spermatogenesis). GnRH is synthesized and secreted by a small number of neuroendocrine neurons, the so-called GnRH neurons. Studies on large animals such as sheep, allowed serial blood sampling from portal vessels in conscious animals and revealed that GnRH secretion was pulsatile and that every LH pulse was preceded by a GnRH pulse (Levine et al. 1982 [17], Clarke et al. 1982 [7], Caraty and al. in 1982 [6]).

Understanding the mechanisms underlying this pulsatility of secretion is one key-clue for the comprehension of infertility linked to hypothalamic dysfunctions. GnRH-neurons are dispersed in the anterior hypothalamus and in situ and simultaneous measurement of numerous neurons cannot be achieved. In vitro approaches have allowed to decipher part of some electrophysiological mechanisms [20, 26], showing the existence of periodic synchronization of electrical activity (see Moenter 2010 [20] for a review), intracellular calcium activity correlated with secretion (Constantin et al. 2009 [8], see Wray 2010 [26] for a review). In the present paper, data was obtained from in vitro primary cultures of GnRH neurons derived from mouse embryonic nasal placodes (see Constantin et al. 2009 [8] for biological methodology). In a previous study, Georgelin et al ([12]) showed the existence of a paracrine/ autocrine regulation by endogenous released GnRH on intracellular calcium activity in the neuronal population. The application of a GnRH antagonist blocking the paracrine/autocrine loop abolished high synchronization events between GnRH neurons which can be defined by a great percentage of neurons simultaneously exhibiting a peak of intracellular calcium (calcium event at a time t). This peaks have a duration of several seconds (3-8) and reflect a sustained increase in intracellular calcium. One crucial step in analyzing data is to correctly detect calcium peaks.

Fluctuations on $([Ca^{2+}]_i)$ are recorded as fluorescence signals captured at a given frequency (here 1 acquisition per second). This fluorescence is directly proportional to the amount of intracellular calcium. However, the intensity of fluorescence may present baseline variations due to methodological causes (fading) or environmental causes (pH, temperature...) but also to high frequency and low amplitude variation in intracellular calcium due synaptic input from neurons in the network. It is then important to be able to isolate the real signal from the noise. Fluorescence was quantified at each unit of time as the mean fluorescence intensity F_k measured in each neuron (cell body) N_k identified as a GnRH neuron. This leads to trajectories like the one showed in Figure 1.

The aim of this paper is to improve the detection of so-called calcium events. A $[Ca^{2+}]_i$ peak was detected at time t if the fluorescence value at t was greater or equal to the average value of the 5 previous points plus c_f times the standard deviation of five previous point. This coefficient c_f is empirically fixed by the biologists to separate "true calcium events" of so-called "noisy calcium events" regardless the observed neuron. Because the decision of being a calcium event is strongly linked to this coefficient c_f and will deeply influence the

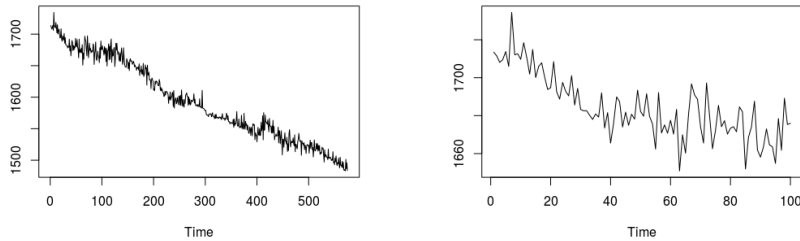


FIGURE 1. Neuronal trajectory from biological data: complete trajectory at left, first 100 values at right.

synchronization analysis, we want to have a robust method to decide whether a peak is an event or not and that could take in account the variability in the fluorescence response. Therefore we proposed a model for the calcium signal and two tests to determine the pics and we will compare them in Section 4.

Inspired by continuous Integrate-And-Fire models (see [5] or [13]), we propose a discrete stochastic model for single recording trajectories. Such a discretization procedure allows us to identify the model with an autoregressive process of order 1 (AR(1)) with a linear trend. Such a model can also be viewed as a linear trend with autoregressive errors and we can use main results developed for time series [3] and especially AR(1) processes. Spiking times are then described through the innovation process.

Several results were proposed to estimate the linear or autoregressive coefficients [22, 24]. We compare here the two main strategies: the first one based on a global contrast function and the second one (called two step estimation) based on a first estimation of the trend followed by the regression coefficient estimate on the detrended series in the spirit of [23]. Then this allows us to get access to estimated innovations, corresponding to a Gaussian mixture with two components with identical standard deviation. Therefore we can use classical mixture estimation [19] and devoted package (`fitgmdist` in Matlab and `Mclust` in R [10]) to estimate parameters and the two classes of times: those that are spiking times and those that are not. Hence we propose several tests for spiking times and compare their sensitivity/specificity on simulated trajectories and show their relevance compared to the initial strategy.

The paper is organized as follows. In Section 2 we describe the parametric model and explain the role of each parameters in link with our biological context. We set and study estimators in Section 3. We obtain explicit asymptotic variance and compare two strategies on some numerical simulations. Section 4 is devoted to our different test strategies, whose efficiency is compared using ROC curves on simulated data. We conclude this paper by several examples from biological experiments. Some numerical illustrations and technical proofs are postponed to an Appendix section.

2. MODEL

2.1. Discrete model. In our biological context, the fluctuation of the calcium concentration is due on one hand to natural clearance and on this other to sudden supplies released from the Reticulum. But ionic channels near the membrane of neurons can provided puffs of calcium and one has to consider also that indirect measurement can provide experimental noise. Moreover, a lot of experiments exhibit a more or less linear trend (see Section 5) probably due to the response fatigue of the fluorescence.

In a continuous setting, several models for spiking neurons like stochastic leaky integrate-and-fire models [5] have been proposed. In their simplest form are solutions of the diffusion equation (see [15]):

$$dX_t = \frac{1}{\tau}(\mu(t) - X_t)dt + \lambda dN_t + \sigma dW_t,$$

where μ is a time inhomogeneous input, W a Brownian motion and N an homogeneous Poisson process independent from W . Since our observed data are recording in a discrete sampling with a constant step time and in order to take every phenomenon in account, we consider a kind of discrete version obtained from an

infill scheme for this model (see Section 6.1 for more details). Hence we assume to observe the $n \geq 1$ points of the following autoregressive process with linear trend:

$$(1) \quad \forall k \in \{0, \dots, n-1\}, \quad X_{n,k+1} = \phi X_{n,k} + a + bk/n + \lambda U_{k+1} + \sigma \varepsilon_{k+1}$$

where

- $\phi \in [0, 1)$ is the coefficient of the autoregressive process, linked to the clearance of the calcium;
- $a \in \mathbb{R}$ and $b \in \mathbb{R}$ correspond to the coefficients of the linear drift.
- $(U_k)_{k \in \{1, \dots, n\}}$ represents the jump times (instants of release from the Reticulum) : it is a family of iid random variables with common distribution $\mathcal{B}(\nu)$ for some $\nu \in [0, 1)$, the jump rate; the jump size is given by $\lambda \in (0, +\infty)$.
- $(\varepsilon_k)_{k \in \{1, \dots, n\}}$ represents the experimental noise or stochastic flux from the channels at the membrane with ratio given by $\sigma \in (0, +\infty)$: it is a family of iid random variables with common distribution $\mathcal{N}(0, 1)$.

Let us remark that we have simplified the Poisson process giving spiking times by a simple Bernoulli sequence. This approximation may be justify when the lapse time of acquisition is very short. Actually, considering an homogeneous Poisson point process of intensity $\mu > 0$, the interspiking duration is given by iid exponential random variables of parameter μ such that their entire upper part is given by iid geometrical random variables of parameter $\nu = 1 - e^{-\mu}$.

We give an illustration of a typical realization of this sequence in Figure 2. In order to understand the effect of the parameters in the the final trajectory we have also plotted the purely jumps one (case without noise nor drift) and the drifted jumps ones (only noise is removed). The initial value X_0 has been chosen as the experimental one observed in Figure 1. Let us emphasize that due to both regression coefficient and noise contributions jumps are not necessarily local maxima of the sample paths.

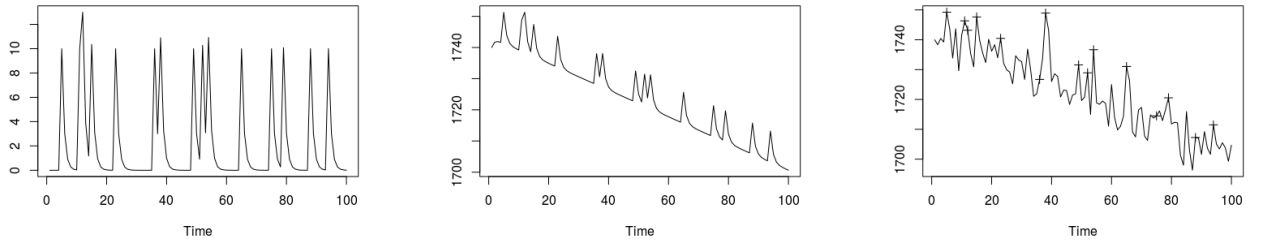


FIGURE 2. One simulation of a trajectory for $\nu = 0.15$, $\lambda = 10$, $\phi = 0.5$, $n = 100$, $X_0 = 520$. From left to right: only the jumps innovations ($\sigma = a = b = 0$), the same jumps innovations with a drift ($a = 1200$, $b = -30$, $\sigma = 0$) the same jumps innovations with a drift and a gaussian noise ($a = 1200$, $b = -30$, $\sigma = 5$): the jumps times are marked with a cross.

The introduction of a and b in the regression equation contributes to a linear trend of the sequence. It will therefore be convenient to assume furthermore that

$$(2) \quad \forall k \in \{0, \dots, n\}, X_{n,k} = Y_k + c_n + dk/n$$

with $(Y_k)_k$ a stationary centered solution of the AR(1) equation

$$(3) \quad Y_{k+1} = \phi Y_k + Z_{k+1},$$

where $(Z_k)_k$ corresponds to the centered innovation that we assume given by

$$Z_k = \lambda(U_k - \nu) + \sigma \varepsilon_k,$$

in such a way that $(Z_k)_k$ is an iid sequence of centered random variables with common variance $\sigma_Z^2 = \lambda^2 \nu(1 - \nu) + \sigma^2$. It follows that the relation between a , b , c_n and d is given by

$$(4) \quad c_n(1 - \phi) + d/n = a + \lambda \nu, \quad d(1 - \phi) = b \text{ iff } c_n = c - \frac{b}{n(1 - \phi)^2}, \quad \text{with } c = \frac{a + \lambda \nu}{1 - \phi} \text{ and } d = \frac{b}{1 - \phi}.$$

Actually, it follows that

$$\begin{aligned}
X_{n,k+1} &= c_n + d \frac{k+1}{n} + Y_{k+1} \\
&= c_n + d \frac{k+1}{n} + \phi Y_k + Z_{k+1} \text{ by (3)} \\
&= \phi X_{n,k} + (1-\phi)c_n + (1-\phi)d \frac{k}{n} + d \frac{1}{n} + Z_{k+1} \text{ by (2)} \\
&= \phi X_{n,k} + (a + \lambda\nu) + b \frac{k}{n} + Z_{k+1},
\end{aligned}$$

so that we get (1). Moreover, denoting $m = a + \lambda\nu$ we may simply rewrite (1) as

$$(5) \quad X_{n,k+1} = \phi X_{n,k} + m + bk/n + Z_{k+1}.$$

The unknown parameters are therefore given by $(a, b, \phi, \lambda, \nu, \sigma)$ or equivalently by $(c, d, \phi, \lambda, \nu, \sigma)$.

Our strategy will consist in first estimating the innovation process $(Z_k)_k$ through the estimation of (m, b, ϕ) and then working on the estimated innovations in order to complete the estimation of the whole parameters and detect times of jumps simply defined as $J_n = \{k \in \{1, \dots, n\}; U_k = 1\}$.

3. PARAMETER ESTIMATION

3.1. Preliminary useful results concerning AR(1) processes. In this section we first give some useful theoretical results when considering $(Y_k)_k$ a stationary centered solution of the AR(1) equation (3) (see [3] for instance). Assuming that $(Z_k)_k$ is an iid sequence with $\mathbb{E}(Z_k) = 0$ and $\text{Var}(Z_k) = \sigma_Z^2 < +\infty$, one can represent $(Y_k)_k$ as a causal MA(∞) process:

$$(6) \quad Y_k = \sum_{n=0}^{+\infty} \phi^n Z_{k-n},$$

where the convergence of the series holds in $L^2(\Omega)$. In particular, it follows that $(Y_k)_k$ is a stationary centered second order process with covariance function given by

$$\rho_Y(k) = \text{Cov}(Y_k, Y_0) = \frac{\phi^{|k|}}{1 - \phi^2} \sigma_Z^2.$$

In order to compute asymptotic variances for the proposed estimators we will need the following results, that we give under general assumptions on innovations since it may be useful for other settings.

Theorem 1. *Let $(Z_k)_k$ be a sequence of iid centered random variables with $\mathbb{E}(Z_0^{4+\delta}) < +\infty$, for some $\delta > 0$, and (Y_k) its associated AR(1) process with autoregression coefficient $\phi \in (-1, 1)$ given by (6). Then we have the following asymptotic normality*

$$\frac{1}{\sqrt{n}} \left(\sum_{k=0}^{n-1} Y_k, \sum_{k=0}^{n-1} \frac{k}{n} Y_k, \sum_{k=0}^{n-1} (Y_k^2 - \rho_Y(0)), \sum_{k=0}^{n-1} Y_k Z_{k+1} \right) \xrightarrow[n \rightarrow +\infty]{d} \mathcal{N}(0, \Sigma_1),$$

with

$$\Sigma_1 = \frac{\sigma_Z^2}{(1-\phi)^2} \begin{pmatrix} 1 & \frac{1}{2} & \frac{\mathbb{E}(Z_0^3)}{(1+\phi)\sigma_Z^2} & 0 \\ \frac{1}{2} & \frac{1}{3} & \frac{\mathbb{E}(Z_0^3)}{2(1+\phi)\sigma_Z^2} & 0 \\ \frac{\mathbb{E}(Z_0^3)}{(1+\phi)\sigma_Z^2} & \frac{\mathbb{E}(Z_0^3)}{2(1+\phi)\sigma_Z^2} & \frac{(\mathbb{E}(Z_0^4) - 3\sigma_Z^4)}{(1+\phi)^2\sigma_Z^2} + 2\sigma_Z^2 \frac{(1+\phi^2)}{(1-\phi)(1+\phi)^3} & \frac{2\sigma_Z^2\phi}{(1+\phi)^2} \\ 0 & 0 & \frac{2\sigma_Z^2\phi}{(1+\phi)^2} & \frac{1-\phi}{1+\phi} \mathbb{E}(Z_0^2) \end{pmatrix}.$$

Let us note that, since our innovations have moments of any order, our assumption on $\mathbb{E}(Z_0^{4+\delta}) < +\infty$ is clearly satisfied. It allows us to use a Central Limit result of [2] for m_n -dependent random variables but it may be weakened with $\mathbb{E}(Z_0^4) < +\infty$. Therefore, we can state the following result under this weaker assumption.

Corollary 1. *Let $(Z_k)_k$ be a sequence of iid centered rv with $\mathbb{E}(Z_0^4) < +\infty$ and (Y_k) its associated AR(1) process with autoregression coefficient $\phi \in (-1, 1)$ given by (6). Then we have the following convergence in L^2 :*

- i) $\frac{1}{n} \sum_{k=0}^{n-1} Y_k \rightarrow 0$ and $\frac{1}{n} \sum_{k=0}^{n-1} \frac{k}{n} Y_k \rightarrow 0$;
- ii) $\frac{1}{n} \sum_{k=0}^{n-1} Y_k^2 \rightarrow \rho_Y(0) = \frac{1}{1-\phi^2} \sigma_Z^2$;

iii) $\frac{1}{n} \sum_{k=0}^{n-1} Y_k Y_{k+1} \rightarrow \rho_Y(1) = \frac{\phi}{1-\phi^2} \sigma_Z^2$ with, denoting $\bar{Y}_n = \frac{1}{n} \sum_{k=0}^{n-1} Y_k$,

$$\frac{1}{\sqrt{n}} \left(\sum_{k=0}^{n-1} [(Y_k - \bar{Y}_n)^2 - \rho_Y(0)], \sum_{k=0}^{n-1} [(Y_k - \bar{Y}_n)(Y_{k-1} - \bar{Y}_n)] - \rho_Y(1) \right) \xrightarrow[n \rightarrow +\infty]{d} \mathcal{N}(0, \Sigma_\rho),$$

with

$$\Sigma_\rho = \rho_Y(0)^2 \begin{pmatrix} (\eta - 3) + 2\frac{1+\phi^2}{1-\phi^2} & \phi \left((\eta - 3) + 2\frac{1+\phi^2}{1-\phi^2} \right) \\ \phi \left((\eta - 3) + 2\frac{1+\phi^2}{1-\phi^2} \right) & (\eta - 3)\phi^2 + 2\frac{1+\phi^2}{1-\phi^2} - (1 + \phi^2) \end{pmatrix},$$

where $\eta = \frac{\mathbb{E}(Z_0^4)}{\sigma_Z^4}$. Hence, for $\hat{\phi}_n := \frac{\sum_{k=0}^{n-1} (Y_k - \bar{Y}_n)(Y_{k+1} - \bar{Y}_n)}{\sum_{k=0}^{n-1} (Y_k - \bar{Y}_n)^2}$ we have

$$\sqrt{n} (\hat{\phi}_n - \phi) \xrightarrow[n \rightarrow +\infty]{d} \mathcal{N}(0, 1 - \phi^2).$$

Proof. In view of the proof of Theorem 1, as soon as $\mathbb{E}(Z_0^4) < +\infty$, we can obtain the convergence of $\sqrt{n}\Sigma_n(Y)$ to Σ_1 where $\Sigma_n(Y)$ is the covariance matrix of $\left(\frac{1}{n} \sum_{k=0}^{n-1} Y_k, \frac{1}{n} \sum_{k=0}^{n-1} \frac{k}{n} Y_k, \frac{1}{n} \sum_{k=0}^{n-1} (Y_k^2 - \rho_Y(0)), \frac{1}{n} \sum_{k=0}^{n-1} Y_k Z_{k+1} \right)$. Then, it implies the corresponding L^2 convergence. Moreover, using the AR(1) equation (3) we write

$$\frac{1}{n} \sum_{k=0}^{n-1} Y_k Y_{k+1} = \phi \frac{1}{n} \sum_{k=0}^{n-1} Y_k^2 + \frac{1}{n} \sum_{k=0}^{n-1} Y_k Z_{k+1} \xrightarrow[n \rightarrow +\infty]{L^2} \phi \rho_Y(0) = \rho_Y(1).$$

The following central limit theorem and ϕ -estimator are classical results (see [3] for instance). Under the assumption that $\mathbb{E}(Z_0^{4+\delta}) < +\infty$, we can recover them thanks to Theorem 1. Actually, since $\bar{Y}_n = O_{\mathbb{P}}\left(\frac{1}{\sqrt{n}}\right)$ the asymptotic normality follows from the fact that

$$\left(\sum_{k=0}^{n-1} [Y_k^2 - \rho_Y(0)], \sum_{k=0}^{n-1} [Y_k Y_{k-1} - \rho_Y(1)] \right)$$

is just a linear transformation of $\left(\sum_{k=0}^{n-1} [Y_k^2 - \rho_Y(0)], \sum_{k=0}^{n-1} Y_k Z_{k-1} \right)$ with corresponding matrix given by $A =$

$\begin{pmatrix} 1 & 0 \\ \phi & 1 \end{pmatrix}$ and we find $\Sigma_\rho = A \Sigma_{3,4}^t A$, where $\Sigma_{3,4}$ denotes the extracted matrix of Σ_1 corresponding to lines and rows number 3 and 4, that corresponds to the asymptotic covariance matrix obtained in Proposition 7.3.4. of [3]. Then using delta-method for $g(x, y) = \frac{y}{x}$ we may prove the asymptotic normality of $\hat{\phi}_n$ with asymptotic variance given by $Dg(\rho_Y(0), \rho_Y(1)) \Sigma_\rho^t Dg(\rho_Y(0), \rho_Y(1))$ where $Dg(\rho_Y(0), \rho_Y(1)) = \frac{1}{\rho_Y(0)} \begin{pmatrix} -\phi & 1 \end{pmatrix}$. \square

Remark 1. Let us mention that these convergence may be strengthened using ergodic properties of $(Y_k)_k$. Actually, according to [1], since the innovation Z_0 has a non trivial absolutely continuous component and $\mathbb{E}(\log(Z_0)^+) < +\infty$, the AR(1) process $(Y_k)_k$ is strong mixing and hence ergodic. Therefore, by the ergodic theorem (see Corollary 9.1.3 of [9] for instance), for any measurable function $g : \mathbb{R} \rightarrow \mathbb{R}$ such that $\mathbb{E}(g(Y_0)^2) < +\infty$ we have

$$\frac{1}{n} \sum_{k=0}^{n-1} g(Y_k) \rightarrow \mathbb{E}(g(Y_0)), \text{ almost surely and in } L^2.$$

Let us also note that these results may be extended to non stationary solutions of the AR(1) equation whatever the initial solution is.

3.2. Estimation of the innovations $(Z_k)_{k \in \{1, \dots, n\}}$.

3.2.1. *Estimation of $m = a + \lambda\nu$, b and ϕ .* In view of (5), we first derive an estimator for $\theta := (m, b, \phi) = (a - \lambda\nu, b, \phi)$ as a contrast based estimator. To this end let us consider the contrast function, defined for $\tilde{\theta} = (\tilde{m}, \tilde{b}, \tilde{\phi}) \in \mathbb{R}^3$ as

$$M_n(\tilde{\theta}) = \sum_{k=0}^{n-1} \left(X_{n,k+1} - \tilde{\phi} X_{n,k} - \tilde{m} - \tilde{b} \frac{k}{n} \right)^2.$$

The minimizer of this quadratic functional is given by

$$(7) \quad \widehat{\theta}_n^{(1)} := ({}^t A_n(X) A_n(X))^{-1} {}^t A_n(X) X = (\widehat{m}_n^{(1)}, \widehat{b}_n^{(1)}, \widehat{\phi}_n^{(1)})$$

where $A_n(X) = \begin{pmatrix} 1 & 0 & X_{n,0} \\ \dots & \dots & \dots \\ 1 & \frac{n-1}{n} & X_{n,n-1} \end{pmatrix}$ is the random matrix of coefficients. Adapting classical proofs for M-estimators (see [25] for instance), we prove the following results (see Appendix).

Theorem 2. *Let us assume that $(X_{n,k})_{0 \leq k \leq n}$ satisfies (5) for some $\theta = (m, b, \phi)$, following from (2), with (Z_k) an iid sequence of centered random variables with $\mathbb{E}(Z_k^4) < +\infty$. Then,*

$$(8) \quad \widehat{\theta}_n^{(1)} := ({}^t A_n(X) A_n(X))^{-1} {}^t A_n(X) X \xrightarrow[n \rightarrow +\infty]{\mathbb{P}} \theta.$$

Moreover,

$$\sqrt{n} \left(\widehat{\theta}_n - \theta \right) \xrightarrow[n \rightarrow +\infty]{d} \mathcal{N}(0, \Sigma_2),$$

where, for $\sigma_Z^2 := \text{Var}(Z_0)$, the matrix Σ_2 is given by

$$\Sigma_2 = \begin{pmatrix} m^2 \frac{1+\phi}{1-\phi} + 4\sigma_Z^2 & mb \frac{1+\phi}{1-\phi} - 6\sigma_Z^2 & -m(1+\phi) \\ mb \frac{1+\phi}{1-\phi} - 6\sigma_Z^2 & b^2 \frac{1+\phi}{1-\phi} + 12\sigma_Z^2 & -b(1+\phi) \\ -m(1+\phi) & -b(1+\phi) & 1-\phi^2 \end{pmatrix},$$

or equivalently, writing $c = \frac{m}{1-\phi}$ and $d = \frac{b}{1-\phi}$, by

$$\Sigma_2 = \begin{pmatrix} c^2 (1-\phi^2) + 4\sigma_Z^2 & cd (1-\phi^2) - 6\sigma_Z^2 & -c (1-\phi^2) \\ cd (1-\phi^2) - 6\sigma_Z^2 & d^2 (1-\phi^2) + 12\sigma_Z^2 & -d (1-\phi^2) \\ -c (1-\phi^2) & -d (1-\phi^2) & 1-\phi^2 \end{pmatrix}.$$

Remark 2. *Let us note that for m and b be fixed, asymptotic variances of $(\widehat{m}_n^{(1)})_n$ and $(\widehat{b}_n^{(1)})_n$ are increasing as ϕ increases to 1, while it is the opposite for c and d be fixed since in this case $m = c(1-\phi)$ and $b = d(1-\phi)$ become smaller with ϕ .*

We check empirically this result for different values of ϕ in Figure 14, postponed to Section 6.4. As expected, in view of the asymptotic variance, the performances are better for ϕ not too close from 1.

3.2.2. Estimation of the trend. Theorem 2 allows us to build an estimator of the parameters $c = \frac{m}{1-\phi}$ and $d = \frac{b}{1-\phi}$ linked with the observed linear trend driven by $c_n = c - \frac{d}{n(1-\phi)}$ and d by considering

$$\widehat{c}_n^{(1)} = \frac{\widehat{m}_n^{(1)}}{1 - \widehat{\phi}_n^{(1)}} - \frac{\widehat{b}_n^{(1)}}{n(1 - \widehat{\phi}_n^{(1)})^2} \text{ and } \widehat{d}_n^{(1)} = \frac{\widehat{b}_n^{(1)}}{1 - \widehat{\phi}_n^{(1)}}.$$

Since $c_n \rightarrow c$, as $n \rightarrow +\infty$, we can deduce from Theorem 2 both consistency and asymptotic normality:

Proposition 1. *Under the assumptions of Theorem 2*

$$\sqrt{n} \left((\widehat{c}_n^{(1)}, \widehat{d}_n^{(1)}, \widehat{\phi}_n^{(1)}) - (c, d, \phi) \right) \xrightarrow[n \rightarrow +\infty]{d} \mathcal{N}(0, \Sigma_3),$$

with

$$(9) \quad \Sigma_3 = \begin{pmatrix} \frac{4\sigma_Z^2}{(1-\phi)^2} & -\frac{6\sigma_Z^2}{(1-\phi)^2} & 0 \\ -\frac{6\sigma_Z^2}{(1-\phi)^2} & \frac{12\sigma_Z^2}{(1-\phi)^2} & 0 \\ 0 & 0 & 1-\phi^2 \end{pmatrix}.$$

Proof. We consider the function from \mathbb{R}^3 to \mathbb{R}^3 defined $\forall (x, y, z) \in \mathbb{R}^3$ by:

$$g(x, y, z) = \left(\frac{x}{1-z}, \frac{y}{1-z}, z \right),$$

such that

$$\sqrt{n} \left((\widehat{c}_n^{(1)}, \widehat{d}_n^{(1)}, \widehat{\phi}_n^{(1)}) - (c, d, \phi) \right) = \sqrt{n} \left(g(\widehat{\theta}_n^{(1)}) - g(\theta) \right) \xrightarrow[n \rightarrow +\infty]{d} \mathcal{N}(0, Dg(\theta) \Sigma_2 {}^t Dg(\theta)).$$

by Theorem 1 and the delta-method ([25]), with

$$Dg(\theta) = \frac{1}{1-\phi} \begin{pmatrix} 1 & 0 & c \\ 0 & 1 & d \\ 0 & 0 & 1-\phi \end{pmatrix}.$$

□

Remark 3. Note that the asymptotic covariance does not depend on c , d and that we get an asymptotic independence between $(\hat{c}_n^{(1)}, \hat{d}_n^{(1)})$ and $\hat{\phi}_n^{(1)}$ in contrast with previous results.

We illustrate this result in Figure 15 (see Section 6.4) and compare for several values of ϕ and σ in Figure 3 below.

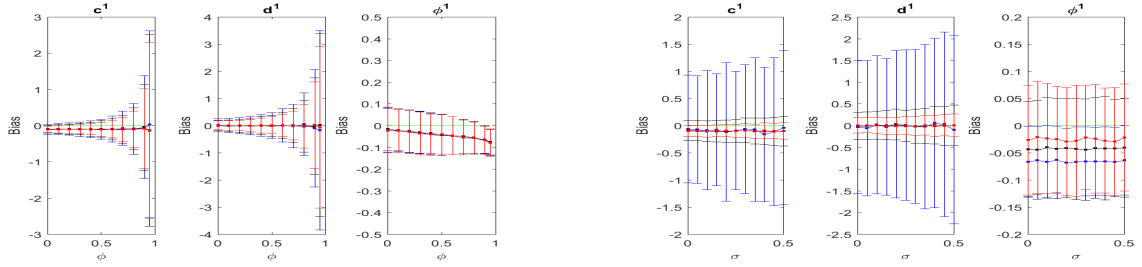


FIGURE 3. Comparison with 1000 simulations, $\nu = 0.3$, $\lambda = 1$, $c = 15$, $d = -10$, $n = 100$, $X_0 = c_n$. On the left: with respect to $\phi \in \{0, 0.1, \dots, 0.9, 0.95\}$, in red $\sigma = 0.1$, in black $\sigma = 0.3$ and in blue $\sigma = 0.5$. On the right with respect to $\sigma \in \{0, 0.05, \dots, 0.5\}$, in red $\phi = 0.1$, in black $\phi = 0.5$ and in blue $\phi = 0.9$

We can notice that, as expected, $\hat{\phi}^{(1)}$ does not depend of the noise σ of the signal, but all the estimators $\hat{c}_n^{(1)}$, $\hat{d}_n^{(1)}$, $\hat{\phi}_n^{(1)}$ depend of ϕ .

Now, a classical way to treat with trend consists in first estimating it and then removing it. When doing so, we have a 2-step estimation procedure by first getting estimators $\hat{c}_n^{(2)}$ and $\hat{d}_n^{(2)}$ given by linear regression of $(X_{n,k})_{0 \leq k \leq n}$ and then computing the autoregression coefficient $\hat{\phi}_n^{(2)}$ by considering the autocorrelation function at lag 1 of the linear regression residuals given by

$$(10) \quad \hat{Y}_{n,k} := X_{n,k} - \hat{c}_n^{(2)} - \hat{d}_n^{(2)}k/n = Y_k + (c_n - \hat{c}_n^{(2)}) + (d - \hat{d}_n^{(2)})k/n.$$

More precisely, by (2) together with the fact that $\frac{1}{n+1} \sum_{k=0}^n \frac{k}{n} = \frac{1}{2}$ and $\frac{1}{n+1} \sum_{k=0}^n \left(\frac{k}{n} - \frac{1}{2}\right)^2 = \frac{n+2}{12n}$, we have for $n > 1$,

$$\begin{aligned} \hat{d}_n^{(2)} &= \frac{12n}{n+2} \times \frac{1}{n+1} \sum_{k=0}^n \left(\frac{k}{n} - \frac{1}{2}\right) (X_{n,k} - \bar{X}_n) \\ &= \frac{12n}{n+2} \times \frac{1}{n+1} \sum_{k=0}^n \left(\frac{k}{n} - \frac{1}{2}\right) \left(Y_k - \bar{Y}_n + d \left(\frac{k}{n} - \frac{1}{2}\right)\right) \end{aligned}$$

where $\bar{X}_n = \frac{1}{n+1} \sum_{k=0}^n X_{n,k}$ and $\bar{Y}_n = \frac{1}{n+1} \sum_{k=0}^n Y_k$, while

$$\begin{aligned} \hat{c}_n^{(2)} &= \bar{X}_n - \frac{1}{2} \hat{d}_n^{(2)} \\ &= c_n + \bar{Y}_n - \frac{1}{2} (\hat{d}_n^{(2)} - d). \end{aligned}$$

It follows that

$$\hat{\phi}_n^{(2)} = \sum_{k=0}^{n-1} (\hat{Y}_{n,k+1} - \bar{Y}_n)(\hat{Y}_{n,k} - \bar{Y}_n) \times \left(\sum_{k=0}^n (\hat{Y}_{n,k} - \bar{Y}_n)^2 \right)^{-1},$$

where $\bar{Y}_n = \frac{1}{n+1} \sum_{k=0}^n \hat{Y}_{n,k}$.

In order to compare with our first estimators we can check that they have the same asymptotic covariance matrix.

Proposition 2. *Let us assume that $(X_{n,k})_{0 \leq k \leq n}$ satisfies (5) for some $\theta = (m, b, \phi)$, following from (2), with (Z_k) an iid sequence of centered random variables with $\mathbb{E}(Z_k^4) < +\infty$ for some $\delta > 0$. Then,*

$$\mathbb{E}(\hat{c}_n^{(2)}) = c_n \quad \text{and} \quad \mathbb{E}(\hat{d}_n^{(2)}) = d.$$

Moreover,

$$\sqrt{n} \left((\hat{c}_n^{(2)}, \hat{d}_n^{(2)}, \hat{\phi}_n^{(2)}) - (c, d, \phi) \right) \xrightarrow[n \rightarrow +\infty]{d} \mathcal{N}(0, \Sigma_3),$$

with Σ_3 given by (9) of Proposition 1.

Proof. We first remark that $\hat{d}_n^{(2)} - d = A_n \cdot S_{n+1}(Y)$, where

$$S_n(Y) = \frac{1}{n} \left(\sum_{k=0}^{n-1} Y_k, \sum_{k=0}^{n-1} \frac{k}{n} Y_k, \sum_{k=0}^{n-1} (Y_k^2 - \rho_Y(0)), \sum_{k=0}^{n-1} Y_k Z_{k+1} \right),$$

have been introduced in Theorem 1 and $A_n = \left(-6 \frac{n}{n+2}, 12 \frac{n+1}{n+2}, 0, 0 \right) \rightarrow A = (-6, 12, 0, 0)$. Therefore $\sqrt{n} (\hat{d}_n^{(2)} - d) \xrightarrow[n \rightarrow +\infty]{d} \mathcal{N}\left(0, \frac{12\sigma_Z^2}{(1-\phi)^2}\right)$, since $A \cdot \Sigma_1 A = \frac{12\sigma_Z^2}{(1-\phi)^2}$ (identifying vectors with column matrices) and $\hat{d}_n^{(2)} - d = O_{\mathbb{P}}(1/\sqrt{n})$. Then, one can remark that for $h \in \{0, 1\}$ we have

$$\frac{1}{n} \sum_{k=0}^{n-1} \left[(\hat{Y}_{n,k+h} - \bar{Y}_n)(\hat{Y}_{n,k} - \bar{Y}_n) - \rho(h) \right] = \frac{1}{n+1} \sum_{k=0}^n Y_{k+h} Y_k - \rho(h) + O_{\mathbb{P}}(1/n),$$

with

$$\sqrt{n} \left(\hat{c}_n^{(2)}, \hat{d}_n^{(2)}, \frac{1}{n+1} \sum_{k=0}^n Y_k^2, \frac{1}{n+1} \sum_{k=0}^n Y_{k+1} Y_k - (c_n, d, \rho(0), \rho(1)) \right) = M_n \sqrt{n} S_{n+1}(Y),$$

for $M_n = \begin{pmatrix} 1 + 3 \frac{n}{n+2} & -6 \frac{n+1}{n+2} & 0 & 0 \\ -6 \frac{n}{n+2} & 12 \frac{n+1}{n+2} & 0 & 0 \\ 0 & 0 & 1 & 0 \\ 0 & 0 & \phi & 1 \end{pmatrix} \xrightarrow[n \rightarrow +\infty]{} M := \begin{pmatrix} 4 & -6 & 0 & 0 \\ -6 & 12 & 0 & 0 \\ 0 & 0 & 1 & 0 \\ 0 & 0 & \phi & 1 \end{pmatrix}$. Since $c_n = c + O(1/n)$, according to Theorem 2 we obtain

$$\sqrt{n} \left(\left(\hat{c}_n^{(2)}, \hat{d}_n^{(2)}, \frac{1}{n} \sum_{k=0}^{n-1} (\hat{Y}_{n,k+1} - \bar{Y}_n)(\hat{Y}_{n,k} - \bar{Y}_n), \frac{1}{n} \sum_{k=0}^{n-1} (\hat{Y}_{n,k} - \bar{Y}_n)^2 \right) - (c, d, \rho(0), \rho(1)) \right) \xrightarrow[n \rightarrow +\infty]{d} \mathcal{N}(0, M \Sigma_1^t M),$$

and the stated result follows by the delta-method. \square

We compare these two procedures in Figure 4. It seems that even for $n = 100$ both behave relatively similarly. This is also the case for larger values of n as illustrated in Figure 18. We only remark that the global estimation seems less biased for ϕ as ϕ is increasing than the 2-Step estimation but its standard deviation is a little bit higher. Let us emphasize that we chose initial conditions in order to be close from the chosen line and we saw that the global estimation was more robust with the choice of initial condition. Let us also remark that as the variance for estimation of ϕ is decreasing with respect $1 - \phi^2$, bias is increasing. Note also that the estimate of c is naturally biased (asymptotically not biased) but the estimate for d seems not too biased.

For comparison we plot the theoretical values of the standard deviation in Figure 5.

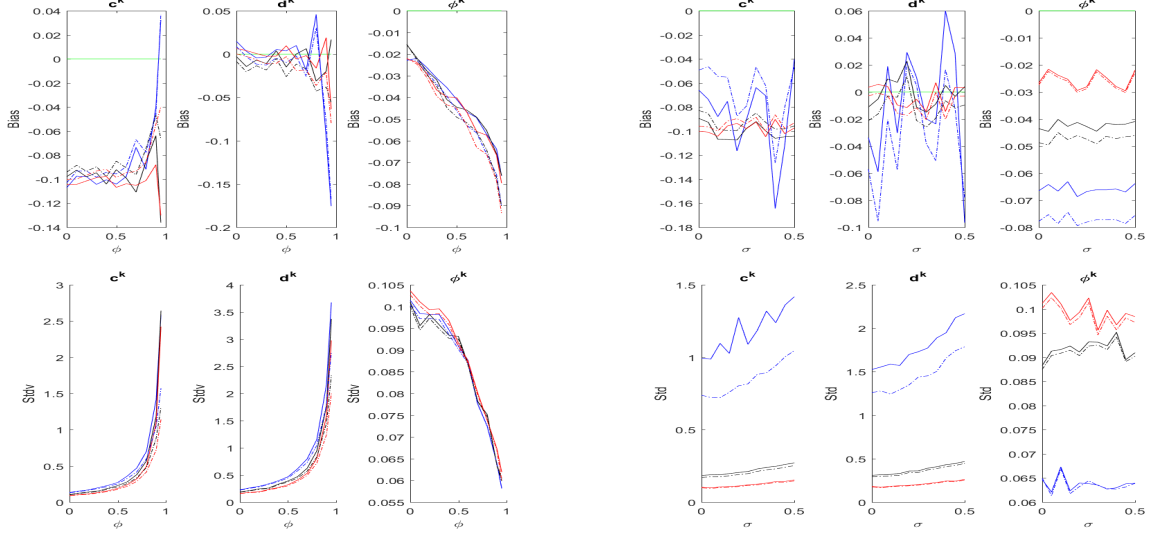


FIGURE 4. Comparison with 1000 simulations, $\nu = 0.3$, $\lambda = 1$, $c = 15$, $d = -10$, $n = 100$, $X_0 = c_n$ with respect to $\phi \in \{0, 0.1, \dots, 0.9, 0.95\}$ on the left and to $\sigma \in \{0, 0.05, \dots, 0.5\}$ on the right. Straight line for the global estimation and dashed line for the 2-step estimation. On the left in red $\sigma = 0.1$, in black $\sigma = 0.3$ and in blue $\sigma = 0.5$. On the right, in red $\phi = 0.1$, in black $\phi = 0.5$ and in blue $\phi = 0.9$.

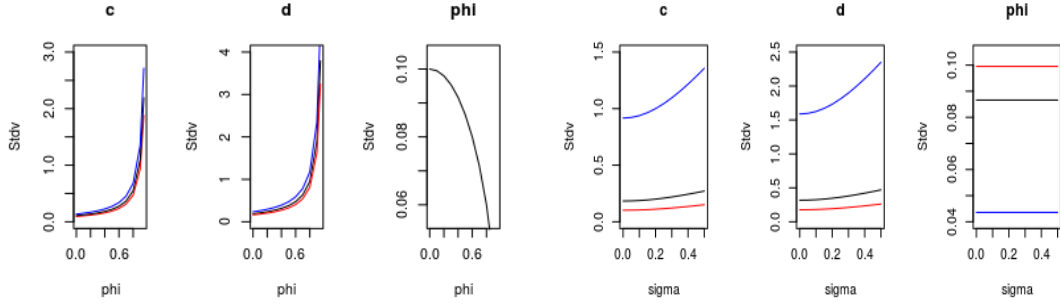


FIGURE 5. Theoretical asymptotic standard deviation for $\nu = 0.3$, $\lambda = 1$, $n = 100$, with respect to $\phi \in \{0, 0.1, \dots, 0.9, 0.95\}$ on the left and to $\sigma \in \{0, 0.05, \dots, 0.5\}$ on the right. On the left in red $\sigma = 0.1$, in black $\sigma = 0.3$ and in blue $\sigma = 0.5$. On the right, in red $\phi = 0.1$, in black $\phi = 0.5$ and in blue $\phi = 0.9$.

3.2.3. *Estimation of the innovations.* Theorem 2 and the 2-step estimation of Proposition 2 provide us two ways for the estimations of innovations $(Z_k)_{k \in \{1, \dots, n\}}$. Namely, we can consider for all $k \in \{1, \dots, n\}$:

$$(11) \quad \widehat{Z}_k^{(1)} = X_{n,k} - \widehat{\phi}_n^{(1)} X_{n,k-1} - \widehat{m}_n^{(1)} - \widehat{b}_n^{(1)} \frac{k-1}{n}$$

or

$$(12) \quad \widehat{Z}_k^{(2)} = \widehat{Y}_{n,k} - \widehat{\phi}_n^{(2)} \widehat{Y}_{n,k-1} \text{ with } \widehat{Y}_{n,k} \text{ given in (10).}$$

Note that, in view of previous results, for all fixed k we have

$$\widehat{Z}_k^{(i)} \xrightarrow[n \rightarrow +\infty]{\mathbb{P}} Z_k.$$

Then, in the sequel, we will explicitly use our assumptions on the distribution of the innovations in order to complete estimation of all the parameters.

3.3. Estimation of λ , ν and σ^2 . Let us recall that we assume that $Z_k = \lambda(U_k - \nu) + \sigma\varepsilon_k$, for $U \sim \mathcal{B}(\nu)$ and $\varepsilon_k \sim \mathcal{N}(0, \sigma^2)$. This implies that Z_k is a mixture between two Gaussian. More precisely, the density of Z_0 is given by

$$f_{Z_0}(z; \psi) = (1 - \nu)\gamma_{-\lambda\nu, \sigma^2}(z) + \nu\gamma_{\lambda(1-\nu), \sigma^2}(z), \text{ for } z \in \mathbb{R}$$

where $\psi := (\nu, \lambda, \sigma)$ and γ_{m, ρ^2} denotes the density of a normal variable of mean m and of variance ρ^2 .

It is classical to use the EM-algorithm to estimate the mixture parameters. We impose that the two components share the same variance and we consider the estimated innovations for all $k \in \{1, \dots, n\}$, $\hat{Z}_k^{(i)}$, for $i = 1$ or 2 . We can use the R function `Mclust` on these estimated innovations [10] or the Matlab function `fitgmdist`, and we impose it two components with the same variance: one for the peaks, the other one for the innovations without peaks. This algorithm gives estimators of the model by iterations of two steps: expectation of the completed log-likelihood of the estimated innovations and choice of parameters which maximize this expectation. At each iteration, the log-likelihood of the estimated innovations increases, which enables us to have a better estimation at a given iteration than at the previous one. We can refer to [21] for more details. The algorithm stops when the log-likelihood increases by increments smaller than a tolerance. It gives us the parameters of the clustering:

- the estimated mean of each gaussian ($\hat{\mu}_1, \hat{\mu}_2$): once sorted such that $\hat{\mu}_1 \leq \hat{\mu}_2$ we should have $\hat{\mu}_1$ that estimates $-\lambda\nu$ and $\hat{\mu}_2$ that estimates $\lambda(1 - \nu)$ so we can use $\hat{\mu}_2 - \hat{\mu}_1$ as an estimator of λ ;
- the estimated proportion of each gaussian (\hat{p}_1, \hat{p}_2): we keep \hat{p}_2 as an estimator of ν ;
- the common estimated variance \hat{v} which estimates σ^2 .

Then we denote by $\hat{\psi}_n^{(i)} := (\hat{\nu}_n^{(i)}, \hat{\lambda}_n^{(i)}, \hat{\sigma}_n^{(i)})$ the corresponding estimators obtained by using $(\hat{Z}_k^{(i)})_{1 \leq k \leq n}$. The main problems of the EM-algorithms are that it not ensures to have the estimator of maximum likelihood if there exist local maxima (importance of the initialization) and that the convergence can be slow. We can refer to [19] to choose the initialization and to [16] to study different types of convergence. Here we use five replicates for each estimation and apply this algorithm with the previous estimated innovation so that we obtain two estimators $\hat{\psi}_n^{(i)} := (\hat{\nu}_n^{(i)}, \hat{\lambda}_n^{(i)}, \hat{\sigma}_n^{(i)})$ for $i = 1, 2$. We present bias as well as empirical 95% confidence intervals in Figure 6, while a specific comparison between global estimation and 2-step estimation for bias and standard deviation is presented in Figure 6.

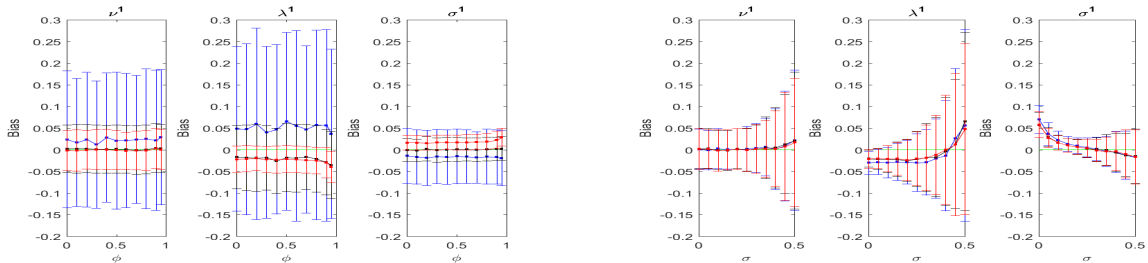


FIGURE 6. Comparison with 1000 simulations, $\nu = 0.3$, $\lambda = 1$, $c = 15$, $d = -10$, $n = 100$, $X_0 = c_n$ for EM estimators using estimated innovations from Theorem 2. On the left: with respect to $\phi \in \{0, 0.1, \dots, 0.9, 0.95\}$, in red $\sigma = 0.1$, in black $\sigma = 0.3$ and in blue $\sigma = 0.5$. On the right with respect to $\sigma \in \{0, 0.05, \dots, 0.5\}$, in red $\phi = 0.1$, in black $\phi = 0.5$ and in blue $\phi = 0.9$

Surprisingly, we notice that the estimators of ν , λ and σ seem not to depend on ϕ , whatever the estimation of the innovations (global or 2-step) and both of them performs rather similarly. We can also remark that here is a stronger bias for the λ estimation and as expected standard deviations increase with respect to σ .

Let us finally remark that we are therefore able to estimate the whole set of parameters since one can then set

$$\hat{a}_n^{(1)} = \hat{m}_n^{(1)} - \hat{\lambda}_n^{(1)}\hat{\nu}_n^{(1)}.$$

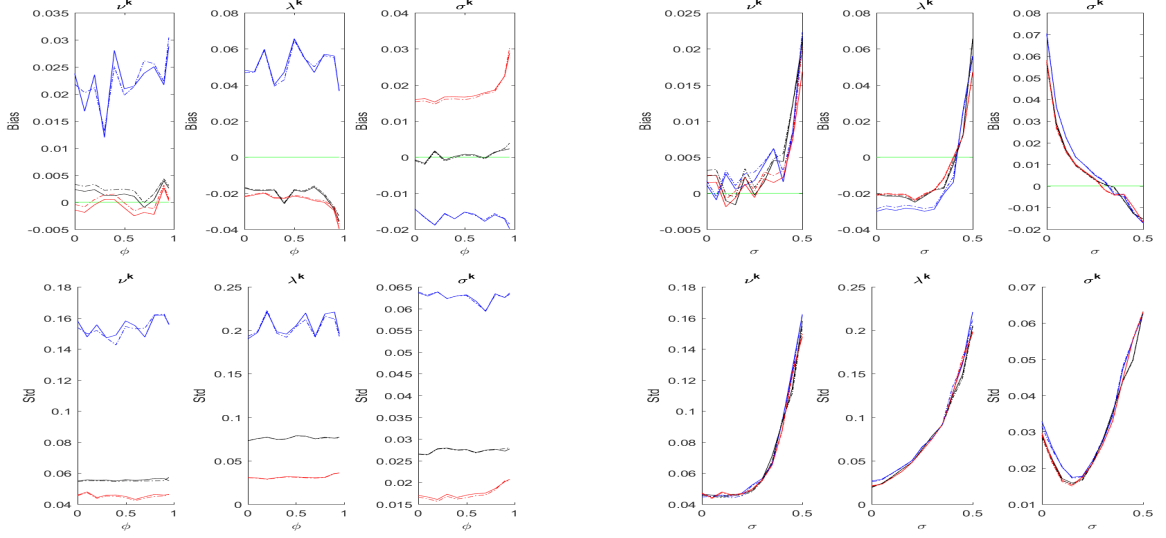


FIGURE 7. Comparison with 1000 simulations, $\nu = 0.3$, $\lambda = 1$, $c = 15$, $d = -10$, $n = 100$, $X_0 = c_n$ with respect to $\phi \in \{0, 0.1, \dots, 0.9, 0.95\}$. Straight line for the global estimation and dashed line for the 2-Step estimation. On the left in red $\sigma = 0.1$, in black $\sigma = 0.3$ and in blue $\sigma = 0.5$. On the right $\phi = 0.1$, in black $\phi = 0.5$ and in blue $\phi = 0.9$.

4. SPIKE DETECTION

Let us recall that the innovations of the process X are given by

$$\forall k \in \{1, \dots, n\}, \quad Z_k = \lambda(U_k - \nu) + \sigma \epsilon_k = X_k - \phi X_{k-1} - a - \lambda \nu - b \frac{k-1}{n},$$

which can be estimated through $\widehat{Z}_k^{(i)}$ where $i = 1$ or 2 . We have already remarked that Z_k is a mixture between two gaussians (see Section 3.3). As we want to detect the spikes, we have to find the $k \in \{1, \dots, n\}$ such that $U_{k+1} = 1$. Therefore we can define two tests.

- T : we consider for a threshold $s \in \mathbb{R}$ the probabilities:

$$P_F := P_F(s, \nu, \lambda, \sigma) = \mathbb{P}(Z_k > s | U_{k+1} = 0) = 1 - \Phi\left(\frac{s + \lambda \nu}{\sigma}\right)$$

$$P_T := P_T(s, \nu, \lambda, \sigma) = \mathbb{P}(Z_k > s | U_{k+1} = 1) = 1 - \Phi\left(\frac{s - \lambda(1 - \nu)}{\sigma}\right),$$

where Φ is the cumulative distribution function of a standard normal variable. We consider also for a tolerance $\alpha \in (0, 1)$:

$$s_\alpha = \min \{s \in \mathbb{R} | P_F \leq \alpha\} = \sigma q_{1-\alpha} - \lambda \nu,$$

where $q_{1-\alpha}$ denotes the quantile of order $1 - \alpha$ of a standard Gaussian random variable. The test T consists in considering the instant k as a peak if $\widehat{Z}_{k+1}^{(i)} > s_\alpha$. Then P_F is the false detection probability at each time k and P_T is the true detection probability at each time k .

- T_c : EM algorithm can provide us the a posteriori probabilities $\mathbb{P}(U_k = 0 | Z_k)$ which are the probabilities, given Z_k , that the instant k is not a peak. Then T_c consists in considering the instant k as a peak if $\mathbb{P}(U_k = 0 | Z_k) < \alpha$, for a tolerance α . Let us quote that the clustering by default is usually given by choosing $\alpha = \frac{1}{2}$.

Then, for $i \in \{1, 2\}$ we denote $T^{(i)}$ and $T_c^{(i)}$ the tests T and T_c , used respectively with the estimations $(\widehat{Z}_k^{(i)})_{1 \leq k \leq n}$.

In order to enlight performances of both tests we consider a trajectory of size $n + 1$ with $n = 100$. We note $(J_k)_{1 \leq k \leq n}$ the sequence of $\{0, 1\}$ -valued variables with true spiking times given by 1 and, for a tolerance α on false detection, $(T_k^{(i)}(\alpha))_{1 \leq k \leq n}$, respectively $(T_{c,k}^{(i)}(\alpha))_{1 \leq k \leq n}$, the sequence of $\{0, 1\}$ -valued variables with detected spiking times given by 1 using estimated innovations $\widehat{Z}_k^{(i)}$ and $\widehat{\psi}_n^{(i)} = (\widehat{\nu}_n^{(i)}, \widehat{\lambda}_n^{(i)}, \widehat{\sigma}_n^{(i)})$, described in the

previous section. Then we can compute

$$\begin{aligned}\tau_T^{(i)}(\alpha) &:= \#\{1 \leq k \leq n; J_k = 1, T_k^{(i)}(\alpha) = 1\} / \#\{1 \leq k \leq n; J_k = 1\}, \\ \tau_F^{(i)}(\alpha) &:= \#\{1 \leq k \leq n; J_k = 0, T_k^{(i)}(\alpha) = 1\} / \#\{1 \leq k \leq n; J_k = 0\},\end{aligned}$$

and similarly we write $\tau_{c,T}^{(i)}(\alpha)$ and $\tau_{c,F}^{(i)}(\alpha)$ when $T^{(i)}$ is replaced by $T_c^{(i)}$.

We present in Figure 17 several realizations obtained considering fixed a, b and with the same jumps. The different values of ϕ contribute to changes in the linear trend and sample paths are very different. In Figure 16 several realizations are obtained considering fixed c, d also with the same jumps. Hence the linear slope is now identical for each realizations and the different values of ϕ only change a little the initial value. Let us emphasize that we chose as initial conditions c_n in order to have a point on the line. This choice corresponds to an ideal case for the 2-step estimations and it performs very similarly than the first global way of estimation. However we have remarked that the global estimation is more robust to changes with respect to initial conditions. We give computed true and false positive rate in Table 4 and Table 3 for a fixed level chosen as $\alpha = 0.01$. We put in bold the minor changes between the two methods of estimation. Whatever the chosen test is, the performances are getting worse as σ is increasing. However, tests T and T_c are not performing similarly for a fixed level. The true and false positive rate for T are higher than for T_c . Despite we have chosen $\alpha = 0.01$ we can obtain up to 0.1 for false positive rate of T , in the worst case $\sigma = 0.5$, while false positive rate of T_c are of the good order.

In order to confirm these first observations we estimate the true and false detection probabilities by considering $N = 1000$ independent simulations of sample paths and computing the empirical mean of the sample

$$(13) \quad \hat{P}_T^{(i)}(\alpha) = \frac{1}{N} \sum_{l=1}^N \left(\tau_T^{(i)}(\alpha) \right)^{(l)} \quad \text{and} \quad \hat{P}_F^{(i)}(\alpha) = \frac{1}{N} \sum_{l=1}^N \left(\tau_F^{(i)}(\alpha) \right)^{(l)},$$

as well as

$$(14) \quad \hat{P}_{c,T}^{(i)}(\alpha) = \frac{1}{N} \sum_{l=1}^N \left(\tau_{c,T}^{(i)}(\alpha) \right)^{(l)} \quad \text{and} \quad \hat{P}_{c,F}^{(i)}(\alpha) = \frac{1}{N} \sum_{l=1}^N \left(\tau_{c,F}^{(i)}(\alpha) \right)^{(l)}.$$

We first present numerical results when ϕ is varying in Figure 8 with also 95% confidence intervals for $\alpha = 0.01$ as previously. Surprisingly, despite the values of ϕ near 1 affect the quality of the first estimated values, it seems to have no consequence on the results of the different tests since their performances do not vary too much with ϕ , as it was also the case for the second estimates using EM-algorithms. However the performances are highly depending on the level of noise σ as we can see in Figure 9 where we have plotted results according to σ varying between 0 and 0.5. As remarked previously, tests are performing similarly choosing the first or the second method of innovations. However as σ is increasing the level of T is higher than α but not exceeding 0.1. In contrast T_c seems to have a lower false detection rate but it has also a lower true detection rate.

A usual way to compare tests is to use ROC curves (for Receiver Operating Characteristic) that enable to measure a binary test's sensitivity. We can refer to [18] for more details. Since our tests depend on a level $\alpha \in (0, 1)$ we can compute empirical ROC curves defined as the location of the pairs $(\hat{P}_F^{(i)}(\alpha), \hat{P}_T^{(i)}(\alpha))$ given by (13) for T or $(\hat{P}_{c,F}^{(i)}(\alpha), \hat{P}_{c,T}^{(i)}(\alpha))$ given by (14) for T_c when α is varying between 0 and 1. Let us quote that we can also compute the theoretical ROC curve associated to T and in this case the pairs (P_F, P_T) are related through the fact that the measure d' defined in [14] by

$$d' = \Phi^{-1}(P_T) - \Phi^{-1}(P_F),$$

where Φ is the cumulative distribution function of a standard normal variable, is constant. With the expressions of P_T and P_F and the symmetry of Φ we obtain $d' = \frac{\lambda}{\sigma}$, so each theoretical curve can be associated to a value of the ratio $\frac{\lambda}{\sigma}$ (and each point of a curve is related to a tolerance α and a threshold s_α). Note that d' increases when P_T increases and when P_F decreases, that is to say when the test is more sensitive and in our case it corresponds to a decrease of σ when λ is constant. This is confirmed by Figure 10 where the area under curve is decreasing with respect to σ increasing in $\{0.1, 0.3, 0.5\}$. The first ROC curve confirms that there is no significant difference between $T^{(1)}$ and $T^{(2)}$ for this kind of simulations. We omit a similar result for $T_c^{(1)}$ and $T_c^{(2)}$. The second ROC curve shows that $T^{(1)}$ seems to be better than $T_c^{(1)}$ and especially as σ is increasing for a fixed $\phi = 0.5$. It reveals that for a rate of false positive detection that we can tolerate, we can find a threshold which provides a bigger rate of true positive detection with $T^{(1)}$ than with $T_c^{(1)}$. This is also true

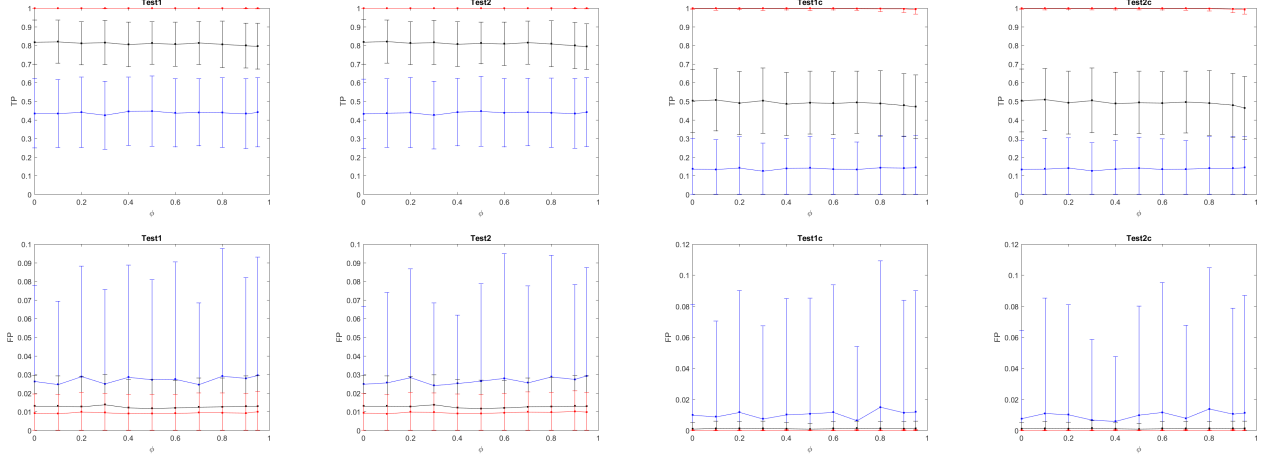


FIGURE 8. Comparison with 1000 simulations, $\nu = 0.3$, $\lambda = 1$, $c = 15$, $d = -10$, $n = 100$, $X_0 = c$ with respect to $\phi \in \{0, 0.1, \dots, 0.9, 0.95\}$. Threshold given by $\alpha = 0.01$. In red $\sigma = 0.1$, in black $\sigma = 0.3$ and in blue $\sigma = 0.5$. First line: True positive rate according to the different Tests. Second line: false positive rate

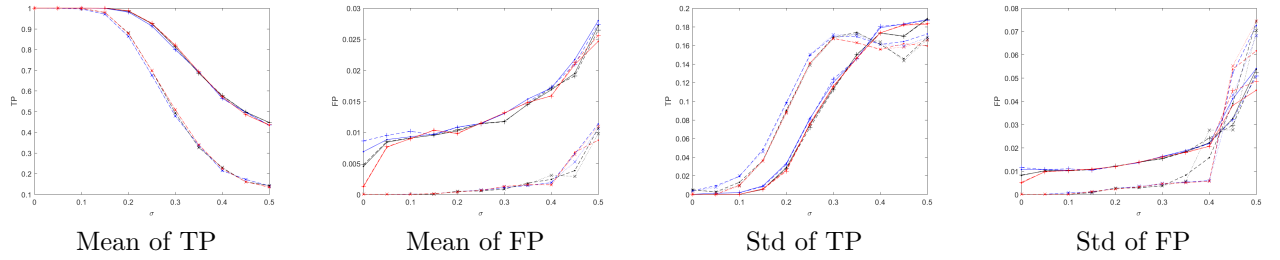


FIGURE 9. Comparison with 1000 simulations, $\nu = 0.3$, $\lambda = 1$, $c = 15$, $d = -10$, $n = 100$, $X_0 = c$ with respect to $\sigma \in \{0, 0.05, \dots, 0.5\}$. Threshold given by $\alpha = 0.01$. In red $\phi = 0.1$, in black $\phi = 0.3$ and in blue $\phi = 0.5$. Straight line with dot for $T^{(1)}$, dashed line with plus for $T^{(2)}$, dashed line with dot for $T_c^{(1)}$, dotted line with cross for $T_c^{(2)}$.

for different values of ϕ since ROC curves completely coincide with ϕ for both tests as shown in the two last figures.

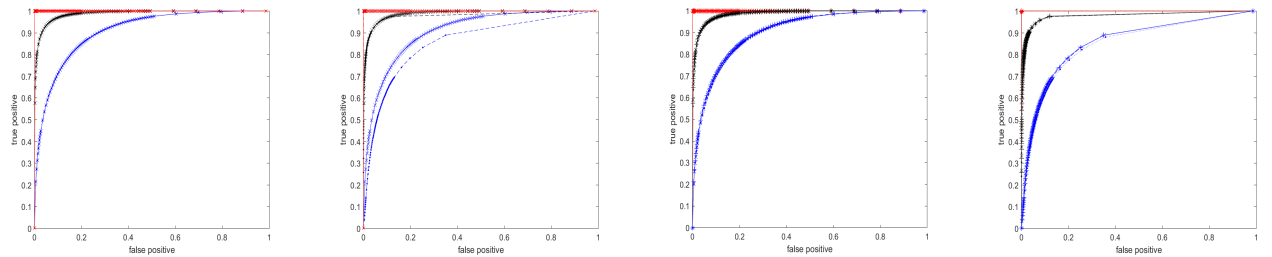


FIGURE 10. ROC curves obtained with 1000 simulations, $\nu = 0.3$, $\lambda = 1$, $c = 15$, $d = -10$, $n = 100$, $X_0 = c_n$. In red $\sigma = 0.1$, in black $\sigma = 0.3$ and in blue $\sigma = 0.5$. First: $\phi = 0.5$, solid line with cross for $T^{(1)}$, dashed line with dot for $T^{(2)}$. Second: $\phi = 0.5$, solid line with cross for $T^{(1)}$, dashed line with dot for $T_c^{(1)}$. Third and Fourth: $T^{(1)}$ (left) and $T_c^{(1)}$ (right) with several values of ϕ , solid line with cross for $\phi = 0.1$, dotted line for $\phi = 0.9$, dashed with plus for $\phi = 0.5$.

5. DATA ANALYSIS

We have considered a biological experiment of Anne Duittoz’s team, composed with 22 trajectories of neurons observed during 575 seconds. More precisely, the observed values correspond to Calcium Green-1 mean fluorescence intensity of 22 selected regions corresponding to neurons in a Calcium imaging recording. For sake of conciseness we only present the two first ones (see Figure 11).

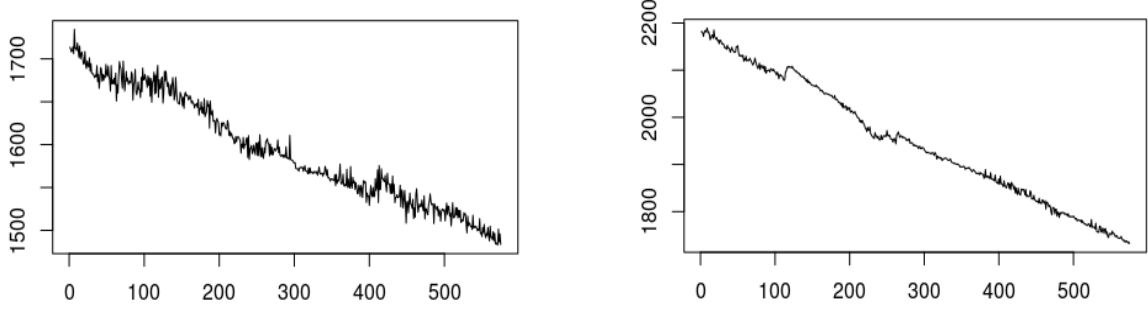


FIGURE 11. Whole trajectory of Neuron 1 and Neuron 2.

In order to apply our spike detection methodology we restrict the time domain to $\{150, \dots, 300\}$. We first obtain estimations of the parameters given in the following table. The results are slightly different according to the first or second estimation but they remain of the same order (see Table 1). Then we apply our different tests for spike detection (see Figure 12). Again, it seems that the tests behave similarly according to the estimation method. However, as already noticed in simulation, the test T_c , based on a posteriori probabilities for EM algorithm, has a less good behavior than the test T with fewer detection and also several ones that do not correspond to local maxima of the sample paths.

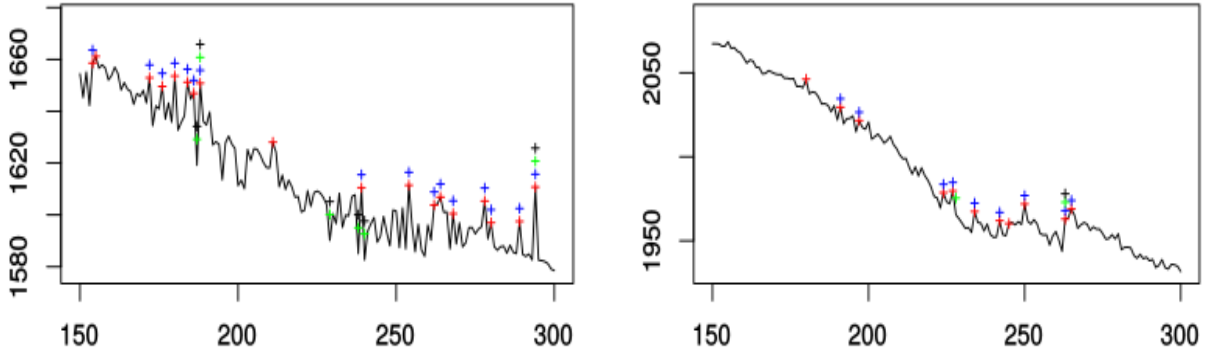


FIGURE 12. Detection of spikes for Neurons 1 and 2 on $\{150, \dots, 300\}$. Threshold given by $\alpha = 0.05$. In red the test $T^{(1)}$, in blue $T^{(2)}$, in green $T_c^{(1)}$, and in black $T_c^{(2)}$.

Neuron	$\hat{\phi}^{(1)}$	$\hat{m}^{(1)}$	$\hat{b}^{(1)}$	$\hat{c}_n^{(1)}$	$\hat{d}^{(1)}$	$\hat{\nu}^{(1)}$	$\hat{\lambda}^{(1)}$	$\hat{\sigma}^{(1)}$
1	0.385	1010	-46.7	1650	-75.9	0.466	1.22	5.4
2	0.923	158	-10.3	2050	-133	0.157	1.47	3.55
	$\hat{\phi}^{(2)}$	$\hat{m}^{(2)}$	$\hat{b}^{(2)}$	$\hat{c}_n^{(2)}$	$\hat{d}^{(2)}$	$\hat{\nu}^{(2)}$	$\hat{\lambda}^{(2)}$	$\hat{\sigma}^{(2)}$
1	0.385	1020	-47.2	1650	-76.7	0.466	1.27	5.37
2	0.916	174	-12	2060	-143	0.137	1.58	3.61

TABLE 1. Estimated parameters for Neurons 1 and 2.

In the whole experiment, we notice a high variability of the estimated parameters between the different neurons, especially for ϕ , as it can be seen in table 2 where the mean value of the estimators, their minimum and maximum obtained from all the neurons of the experience are given.

	$\hat{\phi}^{(1)}$	$\hat{m}^{(1)}$	$\hat{b}^{(1)}$	$\hat{c}_n^{(1)}$	$\hat{d}^{(1)}$	$\hat{\nu}^{(1)}$	$\hat{\lambda}^{(1)}$	$\hat{\sigma}^{(1)}$
mean	0.714	381	-15.1	1340	-59.4	0.455	3.37	3.77
min	0.363	50.4	-46.7	905	-133	0.0747	0.0234	0.966
max	0.946	1010	-1.62	2050	-15.8	0.903	9.3	7.63
	$\hat{\phi}^{(2)}$	$\hat{m}^{(2)}$	$\hat{b}^{(2)}$	$\hat{c}_n^{(i,j),(2)}$	$\hat{d}^{(i,j),(2)}$	$\hat{\nu}^{(2)}$	$\hat{\lambda}^{(2)}$	$\hat{\sigma}^{(2)}$
mean	0.709	388	-15.8	1350	-62.5	0.457	5.16	3.76
min	0.357	50.9	-47.2	906	-143	0.0747	0.511	0.872
max	0.946	1020	-1.98	2060	-15	0.905	18	7.62

TABLE 2. Mean, minimum and maximum of the estimators for the 22 neurons, observed on the time interval $\{150, \dots, 300\}$.

Let us emphasize that the signal- noise ratio $\hat{\lambda}^{(i)}/\hat{\sigma}^{(i)}$ is very low compared to our simulation results. Since the biological interest mainly relies on spikes time interlaps and synchronization events, we should find a good compromise between level confidence and false detection rate and we have therefore chosen a bigger tolerance $\alpha = 0.05$ for the different tests $T^{(1)}$, $T^{(2)}$, $T_c^{(1)}$ and $T_c^{(2)}$. For $\alpha = 0.05$, we have a mean of 17.1% spikes per neuron on the whole time $\{150, \dots, 300\}$ with $T^{(1)}$, 15.3% with $T^{(2)}$, 11.5% with $T_c^{(1)}$ and 12.0% with $T_c^{(2)}$. Now we can consider the influence of the level α by considering, at each time of the experiment, the number of neurons detected to have a spike. For example, with $T^{(1)}$ we give the spike distribution by time in Figure 13 for the level $\alpha = 0.05$ and $\alpha = 0.1$. The time 262 is detected by more than 60% of the neurons and this percentage is not influenced by the level. It is therefore probably a synchronisation event of the experiment.

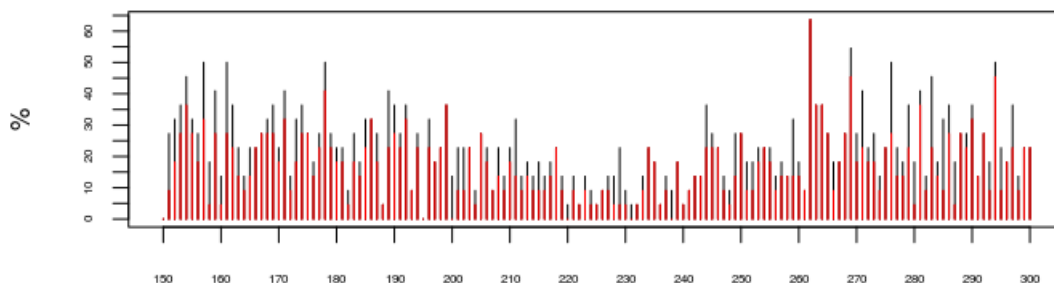


FIGURE 13. Number of spiking neurons with $T^{(1)}$ for each instant between 150 and 300, in red with $\alpha = 0.05$ and in black with $\alpha = 0.1$

In this biological problematic, there are still several issues to work on. In particular, we had to restrict arbitrarily time interval under study to avoid misleading estimates due to heterogeneous parts of the trajectories. This comes from the fact that our simple model does not fit a whole trajectory but can fit some parts with different parameters. It should therefore be necessary to adapt the procedure or the model with a piecewise one in order to mimic data trajectories. Then estimation and detection methods would have to be adapted to this more complex setting, using change-point analysis or sliding window for instance.

6. APPENDIX

6.1. From continuous time to discrete time. We assume to observe a process X over a time interval $[0, T]$, $T \in \mathbb{R}^+$, satisfying

$$dX_t = \frac{1}{\tau}(\mu(t) - X_t)dt + \lambda dN_t + \sigma dW_t,$$

for a linear trend $\mu(t) = c + \frac{d}{T}t$, $c \in \mathbb{R}^+$, $d \in \mathbb{R}$, $\tau, \sigma, \lambda \in (0, +\infty)$, and W a Brownian motion independent from N a Poisson process of parameter $\nu \in (0, 1]$. It follows, writing $\gamma = 1/\tau$ that

$$(15) \quad d(e^{\gamma t} X_t) = \gamma e^{\gamma t} \left(c + \frac{d}{T}t \right) dt + \sigma e^{\gamma t} dW_t + \lambda e^{\gamma t} dN_t.$$

Now, we assume to have $(n+1)$ observations uniformly distributed on $[0, T]$: $X_0, X_{\frac{T}{n}}, \dots, X_{k\frac{T}{n}}, \dots, X_T$. For $k \in \{0, \dots, n\}$, we will note $X_{n,k}$ for $X_{k\frac{T}{n}}$. Moreover, we introduce $\phi_n := e^{-\gamma\frac{T}{n}}$. By integrating (15) over $[k\frac{T}{n}, (k+1)\frac{T}{n}]$, we have:

$$\begin{aligned} \phi_n^{-(k+1)} X_{n,k+1} - \phi_n^{-k} X_{n,k} &= c \left(\phi_n^{-(k+1)} - \phi_n^{-k} \right) + \frac{d}{n} \left((k+1)\phi_n^{-(k+1)} - k\phi_n^{-k} \right) - \frac{d}{\gamma T} \left(\phi_n^{-(k+1)} - \phi_n^{-k} \right) \\ &\quad + \sigma \int_{k\frac{T}{n}}^{(k+1)\frac{T}{n}} e^{\gamma t} dW_t + \lambda \int_{k\frac{T}{n}}^{(k+1)\frac{T}{n}} e^{\gamma t} dN_t. \end{aligned}$$

Or equivalently:

$$\begin{aligned} X_{n,k+1} &= \phi_n X_{n,k} + c(1 - \phi_n) + d\frac{k}{n}(1 - \phi_n) + \frac{d}{n} - \frac{d}{\gamma T}(1 - \phi_n) \\ &\quad + \sigma \int_{k\frac{T}{n}}^{(k+1)\frac{T}{n}} e^{\gamma(t - (k+1)\frac{T}{n})} dW_t + \lambda \sum_{j=N_{k\frac{T}{n}}^{(k+1)\frac{T}{n}}} e^{\gamma(s_j - (k+1)\frac{T}{n})}, \end{aligned}$$

where $(s_j)_j$ are the points of the Poisson process N . Assuming n is large enough:

$$\begin{aligned} \frac{d}{n} - \frac{d}{\gamma T}(1 - \phi_n) &= \frac{d}{n} - \frac{d}{\gamma T} \left(1 - e^{-\gamma\frac{T}{n}} \right) \\ &= \frac{d}{n} - \frac{d}{\gamma T} \left(-\gamma\frac{T}{n} + o\left(\frac{1}{n}\right) \right) \\ &= o\left(\frac{1}{n}\right); \end{aligned}$$

$$\int_{k\frac{T}{n}}^{(k+1)\frac{T}{n}} e^{\gamma(t - (k+1)\frac{T}{n})} dW_t = \left(W_{(k+1)\frac{T}{n}} - W_{k\frac{T}{n}} \right) + o\left(\frac{1}{n}\right),$$

with $W_{(k+1)\frac{T}{n}} - W_{k\frac{T}{n}} \sim \mathcal{N}\left(0, \frac{T}{n}\right)$ and $N_{(k+1)\frac{T}{n}} - N_{k\frac{T}{n}} \sim \mathcal{P}\left(\nu\frac{T}{n}\right)$. Then

$$\mathbb{P}\left(N_{(k+1)\frac{T}{n}} - N_{k\frac{T}{n}} = 1\right) = \nu\frac{T}{n} + o\left(\frac{1}{n}\right) \quad \text{and} \quad \mathbb{P}\left(N_{(k+1)\frac{T}{n}} - N_{k\frac{T}{n}} = 0\right) = 1 - \nu\frac{T}{n} + o\left(\frac{1}{n}\right),$$

so we can consider the following approximation

$$X_{n,k+1} = \phi_n X_{n,k} + c(1 - \phi_n) + d\frac{k}{n}(1 - \phi_n) + \sigma \epsilon_{k+1} + \lambda U_{k+1},$$

where for all $k \in \{0, \dots, n\}$, $\epsilon_k \sim \mathcal{N}\left(0, \frac{T}{n}\right)$, $U_k \sim \mathcal{B}\left(\nu\frac{T}{n}\right)$ are independant variables. In this paper we first consider this approximation for a fix time interlaps $\frac{T}{n} = 1$.

6.2. Proof of Theorem 1. By Cramer-Wold device, it is sufficient to prove that for all u, v, w and x in \mathbb{R} :

$$\frac{1}{\sqrt{n}} \sum_{k=0}^n \Delta_{n,k} \rightarrow \mathcal{N}(0, l),$$

where we denote $\Delta_{n,k} = (u + v + wY_k + xZ_{k+1})Y_k - w\rho_Y(0)$ for all $n \geq 1$ and $k \in \{0, \dots, n\}$ and

$$l = \begin{pmatrix} u & v & w & x \end{pmatrix} \Sigma_1^t \begin{pmatrix} u & v & w & x \end{pmatrix}.$$

As usual for proving asymptotic normality in time series we consider and (m_n) -dependent approximation of (Y_k) defined through $Y_k^{(m_n)} = \sum_{j=0}^{m_n} \phi^j Z_{k-j}$ and denote $\Delta_{n,k}^{(m_n)} = \left(u + v + wY_k^{(m_n)} + xZ_{k+1} \right) Y_k^{(m_n)} - w\rho_{Y^{(m_n)}}(0)$, where $\rho_{Y^{(m_n)}}(0) = \text{Var}(Y_k^{(m_n)})$. Let us remark that we may write

$$\Delta_{n,k} = \Delta_{n,k}^{(m_n)} + \left(u + v\frac{k}{n} + xZ_{k+1} \right) R_{m_n,k} + wR_{m_n,k}^2 + 2wY_k^{(m_n)} R_{m_n,k} + w(\rho_{Y^{(m_n)}}(0) - \rho_Y(0))$$

where $R_{m_n,k} = \sum_{j=m_n+1}^{+\infty} \phi^j Z_{k-j}$. We first notice that for all $\alpha \leq 4 + \delta$

$$\|R_{m_n,k}\|_{L^\alpha} \leq \|Z_0\|_{L^\alpha} \frac{|\phi|^{m_n+1}}{1-|\phi|},$$

which implies that $R_{m_n,k} \rightarrow 0$ in L^α . Let us also remark that since $Y_k^{(m_n)} = \sum_{j=0}^{m_n} \phi^j Z_{k-j}$, we have also $\|Y_k^{(m_n)}\|_{L^\alpha} \leq \frac{1}{1-|\phi|} \|Z_0\|_{L^\alpha}$, by the Minkowski inequality. Moreover,

$$|\rho_Y(0) - \rho_{Y^{(m_n)}}(0)| \leq \sigma_Z^2 \frac{|\phi|^{2(m_n+1)}}{1-\phi^2}.$$

Then we can find $c > 0$ such that $\|\Delta_{n,k} - \Delta_{n,k}^{(m_n)}\|_{L^2} \leq c|\phi|^{m_n}$, so that

$$\left\| \frac{1}{\sqrt{n}} \sum_{k=0}^n (\Delta_{n,k} - \Delta_{n,k}^{(m_n)}) \right\|_{L^2} \leq \sqrt{n} |\phi|^{m_n}.$$

Choosing m_n such that $\sqrt{n}|\phi|^{m_n} \rightarrow 0$, by Slutsky theorem, it is sufficient to prove that

$$\frac{1}{\sqrt{n}} \sum_{k=0}^n \Delta_{n,k}^{(m_n)} \xrightarrow[n \rightarrow +\infty]{d} \mathcal{N}(0, l).$$

For that, since now $(\Delta_{n,k}^{(m_n)})$ is a sequence of m_n -dependent random variables, it is enough to check the four points of the theorem from [2] concerning central limit theorem for m_n dependent random variables. Namely, in our setting, choosing $\delta' = \frac{\delta}{2}$, it follows from

- (i) $\frac{m_n^{2+\frac{2}{\delta'}}}{n}$ converges to 0
- (ii) $\|\Delta_{n,k}^{(m_n)}\|_{L^{2+\delta'}} < +\infty$
- (iii) for some $C > 0$, $\text{Var} \left(\sum_{k=i+1}^j \Delta_{n,k}^{(m_n)} \right) \leq C(j-i)$
- (iv) $\frac{1}{n} \text{Var} \left(\sum_{k=0}^n \Delta_{n,k}^{(m_n)} \right)$ converges to a non-zero limit l .

The first point (i) is simply obtained by choosing $m_n = n^\eta$ for some η such as

$$\eta < \frac{1}{2(1+\frac{1}{\delta'})},$$

so we can take such a value for m_n and remark that $\sqrt{n}|\phi|^{m_n} \rightarrow 0$. Then, for the second point (ii), we first get $\|Z_{k+1} Y_k^{(m_n)}\|_{L^{2+\delta'}} \leq \|Z_{k+1}\|_{L^{4+\delta}} \|Y_k^{(m_n)}\|_{L^{4+\delta}}$, by Cauchy-Schwarz inequality. On the other hand, using again Cauchy-Schwarz inequality, $(Y_k^{(m_n)})^2 \leq \frac{1}{1-|\phi|} \sum_{j=0}^{m_n} |\phi|^j Z_{k-j}^2$ so that

$$\begin{aligned} \|Y_k^{(m_n)2}\|_{L^{2+\delta'}} &\leq \frac{1}{(1-|\phi|)^2} \|Z_0^2\|_{L^{2+\delta'}} \\ &\leq \frac{1}{(1-|\phi|)^2} \|Z_0\|_{L^{4+\delta}}^2 \\ &< +\infty. \end{aligned}$$

Hence, by triangular inequality,

$$\begin{aligned} \|\Delta_{n,k}^{(m_n)}\|_{L^{2+\delta'}} &= \left\| \left(u + v \frac{k}{n} + x Z_{k+1} \right) Y_k^{(m_n)} + w Y_k^{(m_n)2} \right\|_{L^{2+\delta'}} \\ &\leq (|u| + |v|) \|Y_k^{(m_n)}\|_{L^{2+\delta'}} + |x| \|Z_{k+1}\|_{L^{4+\delta}} \|Y_k^{(m_n)}\|_{L^{4+\delta}} + |w| \|Y_k^{(m_n)2}\|_{L^{2+\delta'}} \\ &< +\infty, \end{aligned}$$

that proves point (ii).

For the last two points and in order to get an explicite covariance matrix we need the following intermediate results.

Lemma 1. *Let $(Z_k)_k$ be a sequence of iid centered rv with $\mathbb{E}(Z_0^4) < +\infty$ and (Y_k) its associated AR(1) process with autoregression coefficient $\phi \in (-1, 1)$. Then, for all $n \geq 1$ and $k, l \in \{0, \dots, n-1\}$ we have*

$$\begin{aligned} (1) \quad \text{Cov}(Y_k, Y_l^2) &= \frac{\mathbb{E}(Z_0^3)}{1-\phi^3} \phi^{\frac{1}{2}(l-k) + \frac{3}{2}|l-k|}, \\ (2) \quad \text{Cov}(Y_k, Y_l Z_{l+1}) &= 0, \\ (3) \quad \text{Cov}(Y_k Z_{k+1}, Y_l Z_{l+1}) &= \frac{\sigma_Z^2}{1-\phi^2} \mathbb{E}(Z_0^2) \mathbf{1}_{\{k=l\}}, \\ (4) \quad \text{Cov}(Y_k^2, Y_l Z_{l+1}) &= 2 \frac{\sigma_Z^4}{1-\phi^2} \phi^{2(k-l)-1} \mathbf{1}_{\{k \geq l+1\}}, \\ (5) \quad \text{Cov}(Y_k^2, Y_l^2) &= \text{Cov}(Y_k^2, Y_l^2) = \frac{\sigma_Z^4}{1-\phi^2} \left(\frac{\phi^{2|l-k|} (\mathbb{E}(Z_0^4) - 3\sigma_Z^4)}{\sigma_Z^4(1+\phi^2)} + \frac{2\phi^{2|l-k|}}{1-\phi^2} \right). \end{aligned}$$

It follows that one can find a constant $c > 0$ such that

$$|\text{Cov}(\Delta_{n,k}, \Delta_{n,k})| \leq c|\phi|^{|k-l|}.$$

Moreover, one can choose $c > 0$ such that we also have

$$|\text{Cov}(\Delta_{n,k}^{(m_n)}, \Delta_{n,k}^{(m_n)})| \leq c|\phi|^{|k-l|}.$$

Proof. We first consider k and l such that $0 \leq k \leq l \leq n-1$:

$$(1) \quad \text{Cov}(Y_k, Y_l^2) = \sum_{m,n,p=0}^{+\infty} \phi^{m+n+p} \mathbb{E}(Z_{k-m} Z_{l-n} Z_{l-p}).$$

Since the centered variables Z_k are i.i.d., the terms of this sum are equal to zero except if the indices $k-m$, $l-n$ and $l-p$ are equal then if $p = n = l - k + m$. So we have:

$$\begin{aligned} \text{Cov}(Y_k, Y_l^2) &= \sum_{m=0}^{+\infty} \phi^{3m+2(l-k)} \mathbb{E}(Z_{k-m}^3) \\ &= \frac{\mathbb{E}(Z_0^3)}{1-\phi^3} \phi^{2(l-k)}, \end{aligned}$$

and we note that $|\text{Cov}(Y_k^{m_n}, (Y_l^{m_n})^2)| \leq \frac{\mathbb{E}(|Z_0|^3)}{1-|\phi|^3} |\phi|^{2(l-k)}$.

(2) Since Z_{l+1} is independant of $Y_k Y_l$, we get $\text{Cov}(Y_k, Y_l Z_{l+1}) = 0$ and similarly $\text{Cov}(Y_k^{m_n}, Y_l^{m_n} Z_{l+1}) = 0$.

(3) Since Z_{l+1} is independant of $Y_k Y_l Z_{k+1}$ if $k < l$, we have

$$\begin{aligned} \text{Cov}(Y_k Z_{k+1}, Y_l Z_{l+1}) &= \mathbb{E}(Y_k Z_{k+1} Y_l Z_{l+1}) \mathbf{1}_{\{k=l\}} \\ &= \mathbb{E}(Y_k^2 Z_{k+1}^2) \mathbf{1}_{\{k=l\}} \\ &= \mathbb{E}(Y_k^2) \mathbb{E}(Z_{k+1}^2) \mathbf{1}_{\{k=l\}} \\ &= \frac{\sigma_Z^4}{1-\phi^2} \mathbf{1}_{\{k=l\}}, \end{aligned}$$

and similarly $|\text{Cov}(Y_k^{m_n} Z_{k+1}, Y_l^{m_n} Z_{l+1})| \leq \frac{\sigma_Z^4}{1-|\phi|^2} \mathbf{1}_{\{k=l\}}$.

(4) Since Z_{l+1} is independant of $Y_k^2 Y_l$, we obtain $\text{Cov}(Y_k^2, Y_l Z_{l+1}) = 0 = \text{Cov}((Y_k^{m_n})^2, Y_l^{(m_n)} Z_{l+1})$.

(5) We have

$$\text{Cov}(Y_k^2, Y_l^2) = \sum_{m,n,p,q=0}^{+\infty} \phi^{m+n+p+q} \mathbb{E}(Z_{k-m} Z_{k-n} Z_{l-p} Z_{l-q}) - \rho_Y(0)^2.$$

The terms of this sum are equal to zero except if the indices $k-m$, $k-n$, $l-p$, $l-q$ are all equal or equal in twos, then we deduce that

$$\text{Cov}(Y_k^2, Y_l^2) = \frac{\sigma_Z^4}{1-\phi^2} \left(\frac{\phi^{2(l-k)} (\mathbb{E}(Z_0^4) - 3\sigma_Z^4)}{\sigma_Z^4(1+\phi^2)} + \frac{2\phi^{2(l-k)}}{1-\phi^2} \right),$$

and similarly, one can find $c > 0$ such that $|\text{Cov}((Y_k^{m_n})^2, (Y_l^{m_n})^2)| \leq c|\phi|^{2(l-k)}$.

Now if we have $0 \leq l < k \leq n-1$, we can check the equalities (3) and (5) using symmetric property. For the other ones:

(1)

$$\text{Cov}(Y_k, Y_l^2) = \sum_{m,n,p=0}^{+\infty} \phi^{m+n+p} \mathbb{E}(Z_{k-m} Z_{l-n} Z_{l-p}).$$

The terms of this sum are equal to zero except if the indices $k-m$, $l-n$ and $l-p$ are equal then if $p=n$ and $m=n+k-l$.

$$\text{Cov}(Y_k, Y_l^2) = \sum_{n=0}^{+\infty} \phi^{3n+k-l} \mathbb{E}(Z_{k-l}^3) = \frac{\mathbb{E}(Z_0^3)}{1-\phi^3} \phi^{k-l},$$

while $|\text{Cov}(Y_k^{m_n}, (Y_l^{m_n})^2)| \leq \frac{\mathbb{E}(|Z_0|^3)}{1-|\phi|^3} |\phi|^{k-l}$.

(2)

$$\begin{aligned} \text{Cov}(Y_k, Y_l Z_{l+1}) &= \sum_{m,n=0}^{+\infty} \phi^{m+n} \mathbb{E}(Z_{k-m} Z_{l-n} Z_{l+1}) \\ &= 0 \end{aligned}$$

since the centered variables Z_{k-m} , Z_{l-n} and Z_{l+1} cannot be all equal and we have the same for $\text{Cov}(Y_k^{m_n}, Y_l^{m_n} Z_{l+1})$.

(4) We can prove by induction that

$$\text{Cov}(Y_k^2, Y_l Z_{l+1}) = 2 \frac{\sigma_Z^4}{1-\phi^2} \phi^{2(k-l)-1}.$$

Actually, for $k=l+1$

$$\begin{aligned} \text{Cov}(Y_{l+1}^2, Y_l Z_{l+1}) &= \text{Cov}((\phi Y_l + Z_{l+1})^2, Y_l Z_{l+1}) \\ &= \phi^2 \text{Cov}(Y_l^2, Y_l Z_{l+1}) + \text{Cov}(Z_{l+1}^2, Y_l Z_{l+1}) + 2\phi \text{Var}(Y_l Z_{l+1}) \\ &= 0 + 0 + 2\phi \text{Var}(Y_l) \text{Var}(Z_{l+1}) \\ &= 2 \frac{\phi}{1-\phi^2} \sigma_Z^4 \end{aligned}$$

which proves the property for $k=l+1$. Now assuming that the result holds for $k>l$ we get

$$\begin{aligned} \text{Cov}(Y_{k+1}^2, Y_l Z_{l+1}) &= \text{Cov}((\phi Y_k + Z_{k+1})^2, Y_l Z_{l+1}) \\ &= \phi^2 \text{Cov}(Y_k^2, Y_l Z_{l+1}) + \text{Cov}(Z_{k+1}^2, Y_l Z_{l+1}) + 2\phi \text{Cov}(Y_k Z_{k+1}, Y_l Z_{l+1}) \end{aligned}$$

As $k>l$, the two last terms are equal to zero and

$$\begin{aligned} \text{Cov}(Y_{k+1}^2, Y_l Z_{l+1}) &= \phi^2 \text{Cov}(Y_k^2, Y_l Z_{l+1}) \\ &= 2 \frac{\sigma_Z^4}{1-\phi^2} \phi^{2(k+1-l)-1}, \end{aligned}$$

which proves using induction that (4) holds for any $k \geq l+1$. Finally, let us quote that expanding

$$\text{Cov}\left((Y_k^{(m_n)})^2, Y_l^{(m_n)} Z_{l+1}\right) = \sum_{m,n,p,q=0}^{m_n} \phi^{m+n+p} \mathbb{E}(Z_{k-m} Z_{k-n} Z_{l-p} Z_{l+1}),$$

we also obtain that for $k>l$,

$$\left| \text{Cov}\left((Y_k^{(m_n)})^2, Y_l^{(m_n)} Z_{l+1}\right) \right| \leq 2 \frac{\sigma_Z^4}{1-|\phi|^2} |\phi|^{2(k-l)-1}.$$

Hence, one can find a constant $c > 0$ such that

$$\left| \text{Cov}\left(\Delta_{n,k}^{(m_n)}, \Delta_{n,l}^{(m_n)}\right) \right| \leq c|\phi|^{k-l} \text{ and } |\text{Cov}(\Delta_{n,k}, \Delta_{n,l})| \leq c|\phi|^{k-l}.$$

□

It follows that

$$\text{Var} \left(\sum_{k=i+1}^j \Delta_{n,k}^{(m_n)} \right) \leq c \sum_{k,l=i+1}^j |\phi|^{|k-l|} \leq \frac{c}{1-|\phi|} (j-i),$$

that proves the point (iii).

For the last point (iv), since $\frac{1}{\sqrt{n}} \sum_{k=0}^n (\Delta_{n,k}^{(m_n)} - \Delta_{n,k}) \rightarrow 0$ in L^2 when $n \rightarrow +\infty$, it is enough to prove that $\frac{1}{n} \text{Var} \left(\sum_{k=0}^n \Delta_{n,k} \right) \xrightarrow{n \rightarrow +\infty} l$. Hence, we compute

$$\begin{aligned} \text{Var} \left(\sum_{k=0}^n \Delta_{n,k} \right) &= \text{Var} \left(\sum_{k=0}^{n-1} \left(u + v \frac{k}{n} + wY_k + xZ_{k+1} \right) Y_k \right) \\ &= \sum_{k,l=0}^{n-1} \text{Cov} \left(\left(u + v \frac{k}{n} + wY_k + xZ_{k+1} \right) Y_k, \left(u + v \frac{l}{n} + wY_l + xZ_{l+1} \right) Y_l \right) \\ &= \frac{1}{n} \sum_{k,l=0}^{n-1} \left(u^2 n + uv(k+l) + v^2 \frac{kl}{n} \right) \text{Cov}(Y_k, Y_l) + (uwn + vwk) \text{Cov}(Y_k, Y_l^2) + (uwn + vwl) \text{Cov}(Y_k^2, Y_l) \\ &+ \frac{1}{n} \sum_{k,l=0}^{n-1} (uxn + vlx) \text{Cov}(Y_k, Y_l Z_{l+1}) + (uxn + vlx) \text{Cov}(Y_k Z_{k+1}, Y_l) + nx^2 \text{Cov}(Y_k Z_{k+1}, Y_l Z_{l+1}) \\ &+ \frac{1}{n} \sum_{k,l=0}^{n-1} xwn \text{Cov}(Y_k^2, Y_l Z_{l+1}) + xwn \text{Cov}(Y_k Z_{k+1}, Y_l^2) + nw^2 \text{Cov}(Y_k^2, Y_l^2). \end{aligned}$$

Now in order to get an explicit asymptotic variance we need the following computations.

Lemma 2. *For $|\phi| < 1$, we have the following behaviors when n tends to $+\infty$:*

- (1) $\sum_{i=0}^n \sum_{j=0}^n \phi^{|j-i|} = n \frac{1+\phi}{1-\phi} + o(n);$
- (2) $\sum_{i=0}^n \sum_{j=0}^n i \phi^{|j-i|} = \frac{n^2}{2} \frac{1+\phi}{1-\phi} + o(n^2);$
- (3) $\sum_{i=0}^n \sum_{j=0}^n ij \phi^{|j-i|} = \frac{n^3}{3} \frac{1+\phi}{1-\phi} + o(n^3);$
- (4) $\sum_{i=0}^n \sum_{j=0}^n \phi^{\frac{1}{2}(j-i) + \frac{3}{2}|j-i|} = n \frac{1+\phi+\phi^2}{1-\phi^2} + o(n);$
- (5) $\sum_{i=0}^n \sum_{j=i+1}^n \phi^{2(j-i)-1} = n \frac{\phi}{1-\phi^2} + o(n);$
- (6) $\sum_{i=0}^n \sum_{j=0}^n i \phi^{\frac{1}{2}(j-i) + \frac{3}{2}|j-i|} = \frac{n^2}{2} \frac{1+\phi+\phi^2}{1-\phi^2} + o(n^2).$

Then we obtain that $\frac{1}{n} \text{Var} \left(\sum_{k=0}^{n-1} \Delta_{n,k} \right) \xrightarrow{n \rightarrow \infty} l$, where

$$\begin{aligned}
l &= u^2 \frac{\sigma_Z^2}{1-\phi^2} \frac{1-\phi}{1+\phi} + uv \frac{\sigma_Z^2}{1-\phi^2} \frac{1+\phi}{1-\phi} + v^2 \frac{\sigma_Z^2}{1-\phi^2} \frac{1+\phi}{3(1-\phi)} + 2uw \frac{\mathbb{E}(Z_0^3)}{\sigma_Z^2(1-\phi^3)} \frac{1+\phi+\phi^2}{1-\phi^2} \\
&+ vv \frac{\mathbb{E}(Z_0^3)}{1-\phi^3} \frac{1+\phi+\phi^2}{2(1-\phi^2)} + w^2 \frac{\sigma_Z^4}{1-\phi^2} \frac{1+\phi^2}{1-\phi^2} \left(\frac{\mathbb{E}(Z_0^4) - 3\sigma_Z^4}{\sigma_Z^4(1+\phi^2)} + \frac{2}{1-\phi^2} \right) \\
&+ 4wx \frac{\sigma_Z^4}{1-\phi^2} \frac{\phi}{1-\phi^2} + x^2 \frac{\sigma_Z^4}{1-\phi^2} \\
&= \frac{\sigma_Z^2}{(1-\phi)^2} \left(u^2 + uv + 2uw \frac{\mathbb{E}(Z_0^3)}{\sigma_Z^2(1+\phi)} + \frac{v^2}{3} + \frac{\mathbb{E}(Z_0^3)}{\sigma_Z^2(1+\phi)} vv \right) \\
&+ \frac{\sigma_Z^2}{(1-\phi)^2} \left(w^2 \left(\frac{\mathbb{E}(Z_0^4) - 3\sigma_Z^4}{\sigma_Z^2(1+\phi)^2} + 2 \frac{\sigma_Z^2(1+\phi^2)}{(1-\phi)(1+\phi)^3} \right) + 4wz \frac{\sigma_Z^2 \phi}{(1+\phi)^2} + z^2 \sigma_Z^2 \frac{1-\phi}{1+\phi} \right) \\
&= (u \ v \ w \ x) \Sigma_1^t (u \ v \ w \ x) \neq 0.
\end{aligned}$$

6.3. **Proof of Theorem 2.** Let us write

$$H_n(X) = {}^t A_n(X) A_n(X) = \begin{pmatrix} n & \sum_{k=0}^{n-1} \frac{k}{n} & \sum_{k=0}^{n-1} X_k \\ \sum_{k=0}^{n-1} \frac{k}{n} & \sum_{k=0}^{n-1} \left(\frac{k}{n}\right)^2 & \sum_{k=0}^{n-1} \frac{k}{n} X_k \\ \sum_{k=0}^{n-1} X_k & \sum_{k=0}^{n-1} \frac{k}{n} X_k & \sum_{k=0}^{n-1} X_k^2 \end{pmatrix}.$$

In view of (2), if $(X_{n,k})$ satisfies (5) for some $\theta = (m, b, \phi) \in \mathbb{R}^2 \times]-1, 1[$, we can write $X_{n,k} = c_n + d \frac{k}{n} + Y_k$ with Y a stationary centered solution of the AR(1) equation (3), namely

$$Y_{k+1} = \phi Y_k + Z_{k+1},$$

and c_n, d are given by (4) ie $c_n = c - \frac{b}{n(1-\phi)^2}$, $d = \frac{b}{1-\phi}$ and $c = \frac{m}{1-\phi}$.

Hence, according to Corollary 1,

$$\begin{aligned}
\frac{1}{n} \sum_{k=0}^{n-1} X_{n,k} &= c_n + d \frac{1}{n} \sum_{k=0}^{n-1} \frac{k}{n} + \frac{1}{n} \sum_{k=0}^{n-1} Y_k \xrightarrow[n \rightarrow +\infty]{L^2} c + d/2, \\
\frac{1}{n} \sum_{k=0}^{n-1} \frac{k}{n} X_{n,k} &= c_n \frac{1}{n} \sum_{k=0}^{n-1} \frac{k}{n} + d \frac{1}{n} \sum_{k=0}^{n-1} \left(\frac{k}{n}\right)^2 + \frac{1}{n} \sum_{k=0}^{n-1} \frac{k}{n} Y_k \xrightarrow[n \rightarrow +\infty]{L^2} c/2 + d/3, \\
\frac{1}{n} \sum_{k=0}^{n-1} X_{n,k}^2 &= c_n^2 + 2c_n d \frac{1}{n} \sum_{k=0}^{n-1} \frac{k}{n} + d^2 \frac{1}{n} \sum_{k=0}^{n-1} \left(\frac{k}{n}\right)^2 + \frac{1}{n} \sum_{k=0}^{n-1} Y_k^2 + 2c_n \frac{1}{n} \sum_{k=0}^{n-1} Y_k + 2d \frac{1}{n} \sum_{k=0}^{n-1} \frac{k}{n} Y_k \\
&\xrightarrow[n \rightarrow +\infty]{L^2} c^2 + d^2/3 + cd + \rho_Y(0),
\end{aligned}$$

with $\rho_Y(0) = \sigma_Z^2/(1-\phi^2)$ as the stationary solution of the AR(1) equation. Therefore

$$\frac{1}{n} H_n(X) \xrightarrow[n \rightarrow +\infty]{L^2} H := \begin{pmatrix} 1 & 1/2 & c + d/2 \\ 1/2 & 1/3 & c/2 + d/3 \\ c + d/2 & c/2 + d/3 & c^2 + d^2/3 + cd + \rho_Y(0) \end{pmatrix}.$$

Now let us consider for $\tilde{\theta} = (\tilde{m}, \tilde{b}, \tilde{\phi}) \in \mathbb{R}^3$, the contrast function

$$M_n(\tilde{\theta}) = {}^t (X_n - A_n(X) \tilde{\theta}) (X_n - A_n(X) \tilde{\theta}) = \sum_{k=0}^{n-1} \left(X_{n,k+1} - \tilde{\phi} X_{n,k} - \tilde{m} - \tilde{b} \frac{k}{n} \right)^2,$$

where $X_n := (X_{n,k+1})_{0 \leq k \leq n-1}$. Let us write $\theta = (m, b, \phi)$ the true parameter such that

$$X_{n,k+1} - \phi X_{n,k} - m - b \frac{k}{n} = Z_{k+1},$$

meaning that $X_n - A_n(X)\theta_0 = Z$ for $Z := (Z_{k+1})_{0 \leq k \leq n-1}$. Then $\hat{\theta}_n = \operatorname{argmin}_{\tilde{\theta} \in \mathbb{R}^3} M_n(\tilde{\theta})$ satisfies $J_n(\hat{\theta}_n) = 0$ for $J_n = \nabla M_n$. But $J_n(\tilde{\theta}) = -2^t A_n(X)(X_n - A_n(X)\tilde{\theta})$ and $J_n(\theta) = J_n(\theta) - J_n(\hat{\theta}_n) = -2H_n(X)(\theta - \hat{\theta}_n)$. On the other hand, since $X_n - A_n(X)\theta = Z$, we get

$$J_n(\theta) = -2 \begin{pmatrix} \sum_{k=0}^{n-1} Z_{k+1} \\ \sum_{k=0}^{n-1} \frac{k}{n} Z_{k+1} \\ \sum_{k=0}^{n-1} X_{n,k} Z_{k+1} \end{pmatrix}.$$

We will prove that $\frac{-1}{2\sqrt{n}} J_n(\theta) \xrightarrow[n \rightarrow \infty]{d} \mathcal{N}(0, \Sigma)$, with $\Sigma = \sigma_Z^2 H$. To this end we use again the Cramer-Wold device (see Proposition 6.3.1 of [3] for instance) and consider for $u, v, w \in \mathbb{R}^3$

$$\frac{1}{\sqrt{n}} \sum_{k=0}^{n-1} \left(u + v \frac{k}{n} + w X_{n,k} \right) Z_{k+1} = \frac{1}{\sqrt{n}} \sum_{k=0}^{n-1} \left((u + c_n w) + (v + dw) \frac{k}{n} + w Y_k \right) Z_{k+1},$$

when $(X_{n,k})$ satisfies (2) for some fixed θ .

The convergence will follow from a Lindeberg condition for triangular array of martingales [4]. Actually, let us write $\Delta_{n,k+1} = \left((u + c_n w) + (v + dw) \frac{k}{n} + w Y_k \right) Z_{k+1}$ and $S_{n,l} = \sum_{k=0}^l \Delta_{n,k+1}$. We may consider the filtration $\mathcal{F}_{n,l} = \sigma(Z_k, k \leq l) = \mathcal{F}_l$. It follows that $\mathbb{E}(\Delta_{n,k+1} | \mathcal{F}_{n,k}) = \mathbb{E}(\Delta_{n,k+1} | \mathcal{F}_k) = \left((u + c_n w) + (v + dw) \frac{k}{n} + w Y_k \right) \mathbb{E}(Z_{k+1}) = 0$ a.s. since Z_{k+1} is centered and independent from \mathcal{F}_k and $(S_{n,l})$ is a martingale triangular array. Then let us write $\frac{S_n}{s_n} := \frac{S_{n,n-1}}{s_n}$, where $s_n^2 = \operatorname{Var}(S_{n,n-1})$. Hence according to Theorem 2 of [4] or [11] if

$$(16) \quad \frac{1}{s_n^2} \sum_{k=1}^{n-1} \mathbb{E}(\Delta_{n,k+1}^2 | \mathcal{F}_k) \xrightarrow[n \rightarrow +\infty]{\mathbb{P}} 1,$$

$$(17) \quad \text{and } \frac{1}{s_n^2} \sum_{k=1}^{n-1} \mathbb{E}(\Delta_{n,k+1}^2 \mathbf{1}_{|\Delta_{n,k+1}| > \varepsilon s_n} | \mathcal{F}_k) \xrightarrow[n \rightarrow +\infty]{\mathbb{P}} 0, \text{ for all } \varepsilon > 0,$$

we have $\frac{S_n}{s_n} \xrightarrow[n \rightarrow +\infty]{d} \mathcal{N}(0, 1)$.

So let us first compute the asymptotic variance. We write $\langle S \rangle_n = \sum_{k=1}^{n-1} \mathbb{E}(\Delta_{n,k+1}^2 | \mathcal{F}_k)$ and note that $s_n^2 = \mathbb{E}(\langle S \rangle_n)$. In our setting, it is clear that

$$\mathbb{E}(\Delta_{n,k+1}^2 | \mathcal{F}_k) = \sigma_Z^2 \left((u + c_n w) + (v + dw) \frac{k}{n} + w Y_k \right)^2.$$

By Corollary 1 we have $\frac{1}{n} \sum_{k=0}^{n-1} Y_k \rightarrow 0$, $\frac{1}{n} \sum_{k=0}^{n-1} \frac{k}{n} Y_k \rightarrow 0$ and $\frac{1}{n} \sum_{k=0}^{n-1} Y_k^2 \rightarrow \rho_Y(0)$ in L^2 and we may deduce that

$$\frac{1}{n} \sum_{k=0}^{n-1} \mathbb{E}(\Delta_{n,k+1}^2 | \mathcal{F}_k) \xrightarrow[n \rightarrow +\infty]{L^2} s^2 := \sigma_Z^2 \left((u + cw)^2 + \frac{1}{3}(v + dw)^2 + w^2 \rho_Y(0) + (u + cw)(v + dw) \right).$$

Hence,

$$\frac{s_n^2}{n} \xrightarrow[n \rightarrow +\infty]{} s^2,$$

and (16) follows writting

$$\frac{1}{s_n^2} \sum_{k=0}^{n-1} \mathbb{E}(\Delta_{n,k+1}^2 | \mathcal{F}_k) = \frac{n}{s_n^2} \times \frac{1}{n} \sum_{k=0}^{n-1} \mathbb{E}(\Delta_{n,k+1}^2 | \mathcal{F}_k).$$

Note that we may deduce from these lines that the asymptotic covariance matrix is given by

$$\Sigma = \sigma_Z^2 \begin{pmatrix} 1 & \frac{1}{2} & c + \frac{d}{2} \\ \frac{1}{2} & \frac{1}{3} & \frac{c}{2} + \frac{d}{3} \\ c + \frac{d}{2} & \frac{c}{2} + \frac{d}{3} & c^2 + \frac{d^2}{3} + \rho_Y(0) + cd \end{pmatrix} = \sigma_Z^2 H.$$

Now it remains to prove the Lindeberg condition (17). So let us fix $N \in \mathbb{N}^*$ large enough such that for all $n \geq 2N$ we have $s_n > s^2\sqrt{N}$, choose $C > 0$ such that $|\Delta_{n,k+1}| \leq C(1 + |Y_k|)|Z_{k+1}|$ and remark that for $n \geq 2N$, we have

$$\begin{aligned} \frac{1}{n} \sum_{k=0}^{n-1} \mathbb{E}(\Delta_{n,k+1}^2 \mathbf{1}_{|\Delta_{n,k+1}| > \varepsilon s_n} | \mathcal{F}_k) &\leq \frac{1}{n} \sum_{k=0}^{n-1} \mathbb{E}(\Delta_{n,k+1}^2 \mathbf{1}_{|\Delta_{n,k+1}| > \varepsilon s\sqrt{N}} | \mathcal{F}_k) \\ &\leq \frac{C^2}{n} \sum_{k=0}^{n-1} \mathbb{E}((1 + |Y_k|)^2 Z_{k+1}^2 \mathbf{1}_{|C(1+|Y_k|)|Z_{k+1}| > \varepsilon s\sqrt{N}} | \mathcal{F}_k). \end{aligned}$$

Hence, by stationarity, we get

$$\mathbb{E} \left(\frac{1}{n} \sum_{k=0}^{n-1} \mathbb{E}(\Delta_{n,k+1}^2 \mathbf{1}_{|\Delta_{n,k+1}| > \varepsilon s_n} | \mathcal{F}_k) \right) = C^2 \mathbb{E}((1 + |Y_0|)^2 Z_1^2 \mathbf{1}_{|(1+|Y_0|)|Z_1| > \varepsilon s\sqrt{N}/C}) \xrightarrow{N \rightarrow +\infty} 0,$$

since $\mathbb{E}((1 + |Y_0|)^2 Z_1^2) < +\infty$, and allows to get (17). We have therefore $\frac{S_n}{s_n} \xrightarrow[n \rightarrow +\infty]{d} \mathcal{N}(0, 1)$ and consequently, by Slutsky's theorem, $\frac{-1}{2\sqrt{n}} J_n(\theta) = \frac{s_n}{\sqrt{n}} \frac{S_n}{s_n} \xrightarrow[n \rightarrow +\infty]{d} \mathcal{N}(0, s^2)$. But $\frac{-1}{2\sqrt{n}} J_n(\theta) = \frac{1}{n} H_n(X) \sqrt{n}(\theta - \hat{\theta}_n)$, and we can write

$$\sqrt{n}(\theta - \hat{\theta}_n) = \left(\frac{1}{n} H_n(X) \right)^{-1} \frac{-1}{2\sqrt{n}} J_n(\theta).$$

Again, by Slutsky's theorem, we may deduce that

$$\sqrt{n}(\theta - \hat{\theta}_n) \longrightarrow H^{-1} \mathcal{N}(0, \Sigma) = \mathcal{N}(0, H^{-1} \Sigma^t H^{-1}) = \mathcal{N}(0, \sigma_Z^2 H^{-1}).$$

Note that $\det(H) = \frac{\rho_Y(0)}{12}$, so

$$\Sigma_2 = \sigma_Z^2 H^{-1} = (1 - \phi^2) \begin{pmatrix} c^2 + 4\rho_Y(0) & cd - 6\rho_Y(0) & -c \\ cd - 6\rho_Y(0) & d^2 + 12\rho_Y(0) & -d \\ -c & -d & 1 \end{pmatrix},$$

with $c = \frac{m}{1-\phi}$, $d = \frac{b}{1-\phi}$ and $\rho_Y(0) = \frac{1}{1-\phi^2} \sigma_Z^2$.

6.4. Numerical results. We first present some histograms obtained with 1000 simulations, $\nu = 0.3$, $\lambda = 1$, $\sigma = 0.2$, and $n = 1000$. The red lines correspond to the theoretical gaussian distribution with variance computed according to Theorem 2.

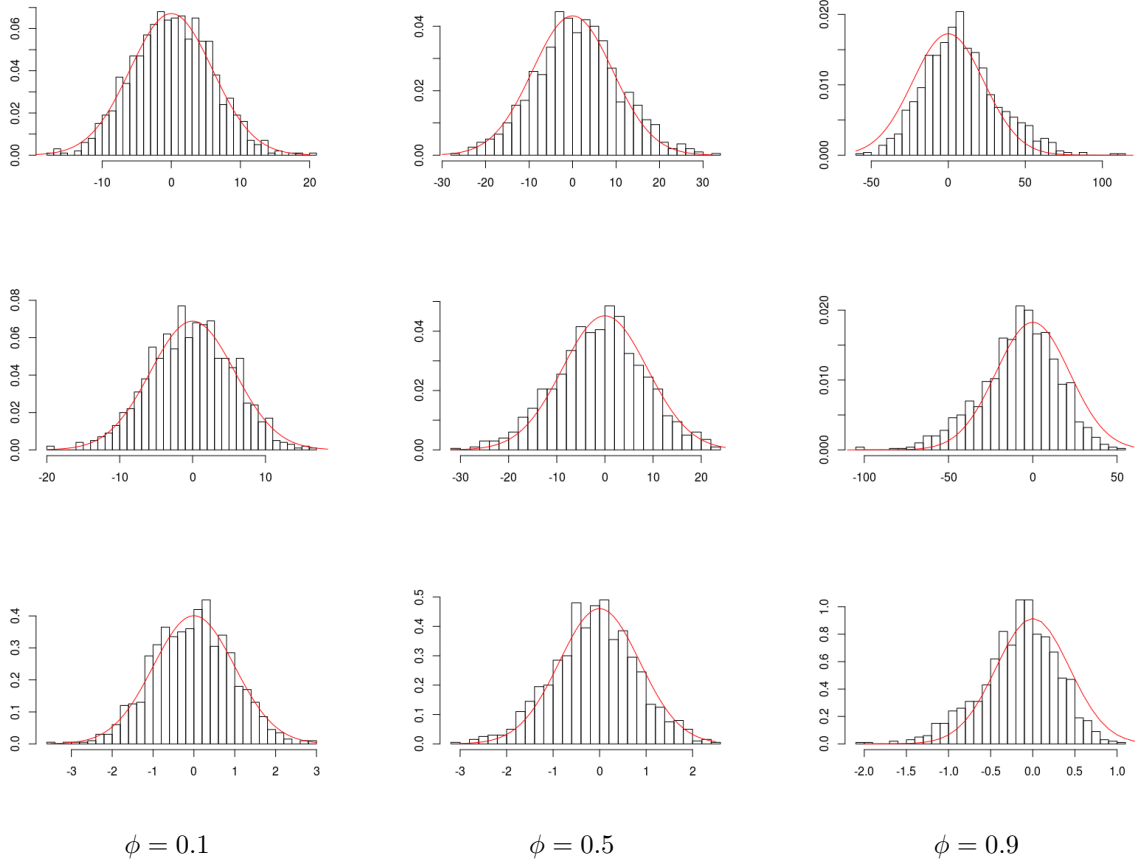


FIGURE 14. Histograms for $a = 5$, $b = -5$. First row: $(\widehat{m}_n^{(1)} - m)$. Second row: $(\widehat{b}_n^{(1)} - b)$. Third row: $(\widehat{\phi}_n^{(1)} - \phi)$.

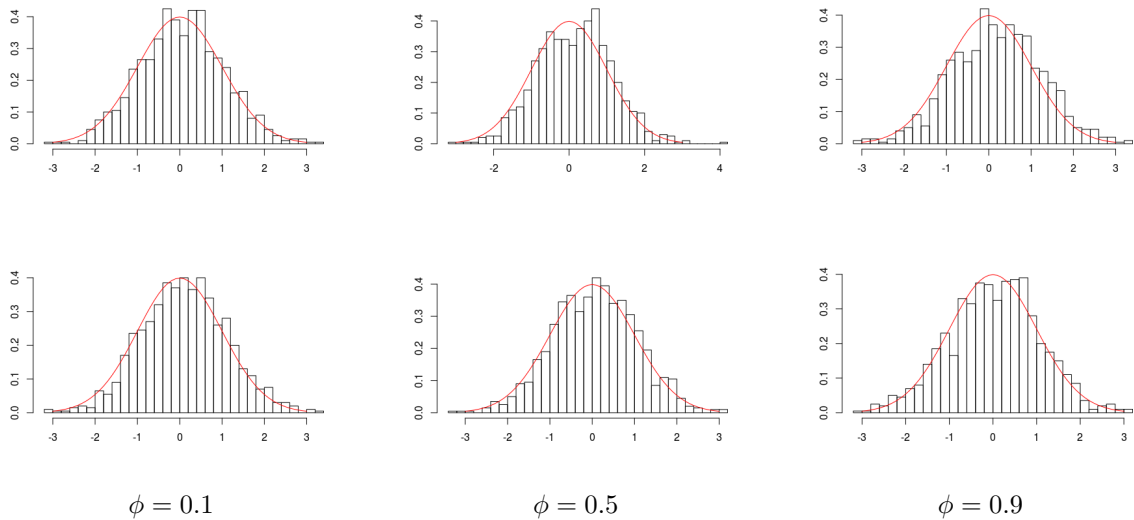


FIGURE 15. Histograms for $c = 5$, $d = -5$, $n = 1000$. First row: $(\widehat{c}_n^{(1)} - c)$. Second row: $(\widehat{d}_n^{(1)} - d)$.

Now we present typical realizations of trajectories for several choices of parameters but with the same jumps (in red star) in order to illustrate the parameters effect on shapes and tests. We set $\nu = 0.3$, $\lambda = 1$, $n = 100$ and consider tests with level $\alpha = 0.01$: in blue cross detected jumps with $T^{(1)}$, in black plus $T_c^{(1)}$, in blue circle with $T^{(2)}$ and in black circle with $T_c^{(2)}$. The red line, respectively green line, is the estimated line with the

first, respectively the second, estimators. The dot black line corresponds to the straight line with parameters (c_n, d) .

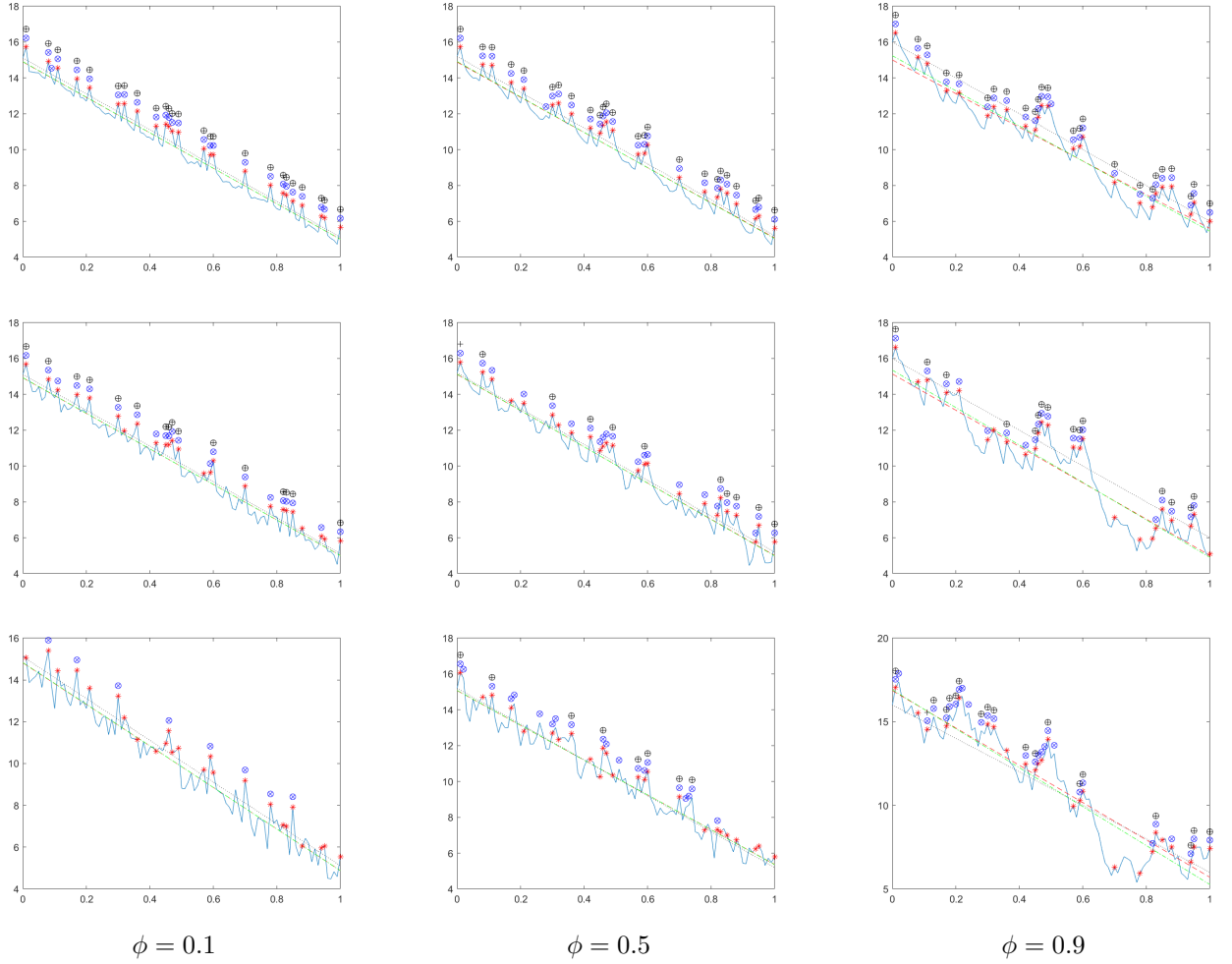


FIGURE 16. Test over one simulation for $c = 15$, $d = -10$, $b = d(1 - \phi)$, $a = c(1 - \phi) - \lambda\nu$, $X_0 = c_n$, with $c_n = c - d/(n(1 - \phi))$. First line: $\sigma = 0.1$, second line: $\sigma = 0.3$, third line: $\sigma = 0.5$.

σ	$\phi = 0.1$				$\phi = 0.5$				$\phi = 0.9$			
	$\tau_T^{(1)}$	$\tau_F^{(1)}$	$\tau_{c,T}^{(1)}$	$\tau_{c,F}^{(1)}$	$\tau_T^{(1)}$	$\tau_F^{(1)}$	$\tau_{c,T}^{(1)}$	$\tau_{c,F}^{(1)}$	$\tau_T^{(1)}$	$\tau_F^{(1)}$	$\tau_{c,T}^{(1)}$	$\tau_{c,F}^{(1)}$
0.1	1	0.013	1	0	1	0.013	1	0	1	0.013	1	0
0.3	0.840	0	0.640	0	0.920	0	0.440	0	0.760	0	0.600	0
0.5	0.320	0	0	0	0.480	0.105	0.280	0.013	0.760	0.118	0.600	0.053
σ	$\tau_T^{(2)}$	$\tau_F^{(2)}$	$\tau_{c,T}^{(2)}$	$\tau_{c,F}^{(2)}$	$\tau_T^{(2)}$	$\tau_F^{(2)}$	$\tau_{c,T}^{(2)}$	$\tau_{c,F}^{(2)}$	$\tau_T^{(2)}$	$\tau_F^{(2)}$	$\tau_{c,T}^{(2)}$	$\tau_{c,F}^{(2)}$
0.1	1	0.013	1	0	1	0.013	1	0	1	0.013	1	0
0.3	0.840	0	0.640	0	0.920	0	0.400	0	0.760	0	0.600	0
0.5	0.320	0	0	0	0.480	0.105	0.280	0.013	0.760	0.118	0.560	0.053

TABLE 3. Test over one simulation for $\nu = 0.3$, $\lambda = 1$, $c = 15$, $d = -10$, $b = d(1 - \phi)$, $a = c(1 - \phi) - \lambda\nu$, $X_0 = c_n$, with $c_n = c - d/(n(1 - \phi))$ and $n = 100$, as shown in Figure 16 with tolerance $\alpha = 0.01$. The number of jumps is 25.

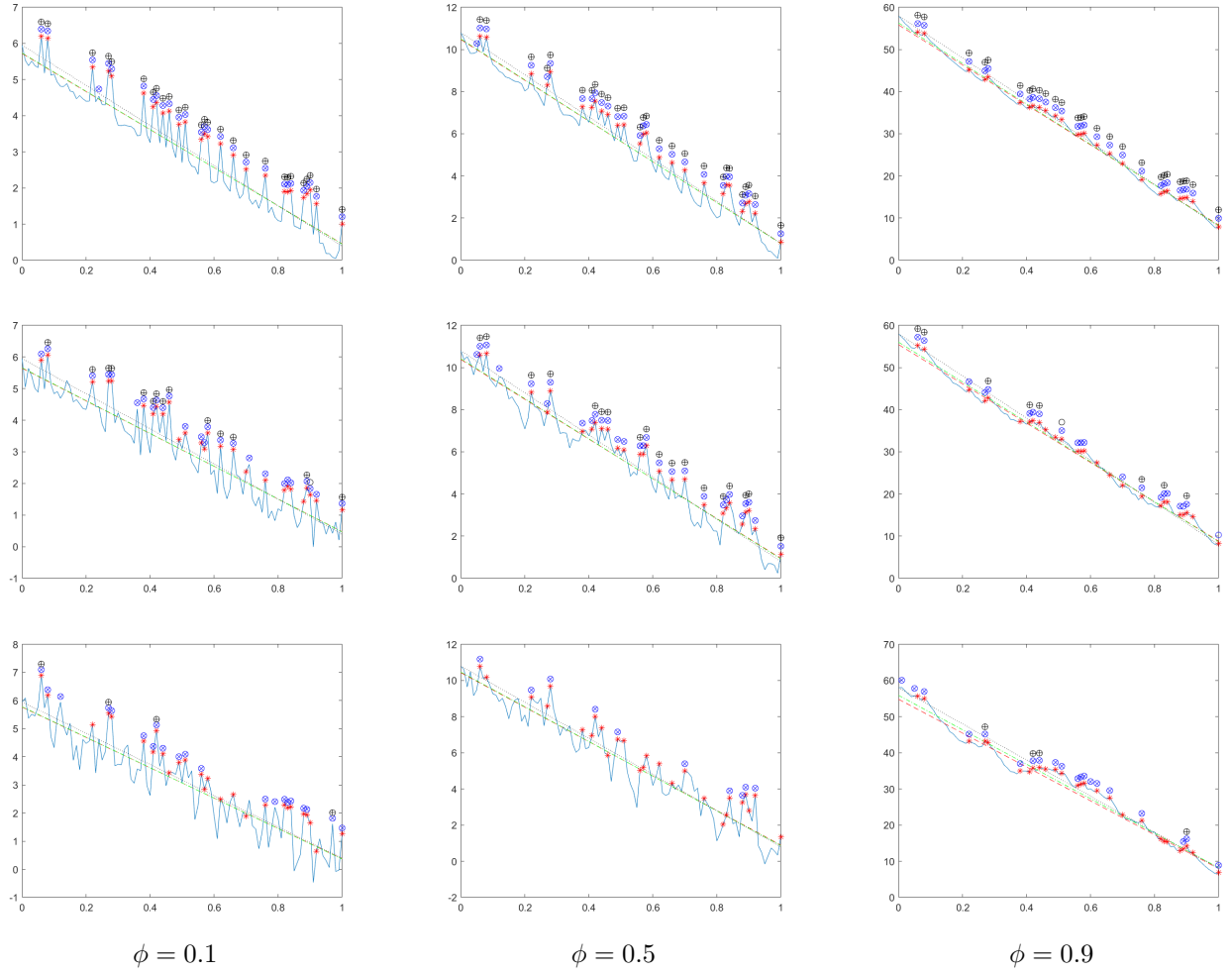


FIGURE 17. Test over one simulation for $a = 5$, $b = -5$, $d = b/(1 - \phi)$, $c_n = (a + \lambda\nu)/(1 - \phi) - b/(n(1 - \phi)^2)$, $X_0 = c_n$. First line: $\sigma = 0.1$, second line: $\sigma = 0.3$, third line: $\sigma = 0.5$.

	$\phi = 0.1$				$\phi = 0.5$				$\phi = 0.9$			
σ	$\tau_T^{(1)}$	$\tau_F^{(1)}$	$\tau_{c,T}^{(1)}$	$\tau_{c,F}^{(1)}$	$\tau_T^{(1)}$	$\tau_F^{(1)}$	$\tau_{c,T}^{(1)}$	$\tau_{c,F}^{(1)}$	$\tau_T^{(1)}$	$\tau_F^{(1)}$	$\tau_{c,T}^{(1)}$	$\tau_{c,F}^{(1)}$
0.1	1	0.014	1	0	1	0.014	1	0	1	0	1	0
0.3	0.889	0.027	0.519	0	1	0.027	0.667	0	0.704	0	0.296	0
0.5	0.667	0.041	0.111	0.014	0.370	0	0	0	0.630	0.041	0.148	0
σ	$\tau_T^{(2)}$	$\tau_F^{(2)}$	$\tau_{c,T}^{(2)}$	$\tau_{c,F}^{(2)}$	$\tau_T^{(2)}$	$\tau_F^{(2)}$	$\tau_{c,T}^{(2)}$	$\tau_{c,F}^{(2)}$	$\tau_T^{(2)}$	$\tau_F^{(2)}$	$\tau_{c,T}^{(2)}$	$\tau_{c,F}^{(2)}$
0.1	1	0.014	1	0	1	0.014	1	0	1	0	1	0
0.3	0.889	0.027	0.556	0	1	0.027	0.667	0	0.778	0	0.333	0
0.5	0.667	0.041	0.111	0.014	0.370	0	0	0	0.630	0.041	0.148	0

TABLE 4. Test over one simulation for $\nu = 0.3$, $\lambda = 1$, $a = 5$, $b = -5$, $d = b/(1 - \phi)$, $c_n = (a + \lambda\nu)/(1 - \phi) - b/(n(1 - \phi)^2)$, $X_0 = c_n$, $n = 100$, as shown in Figure 17 with tolerance $\alpha = 0.01$. The number of jumps is 27.

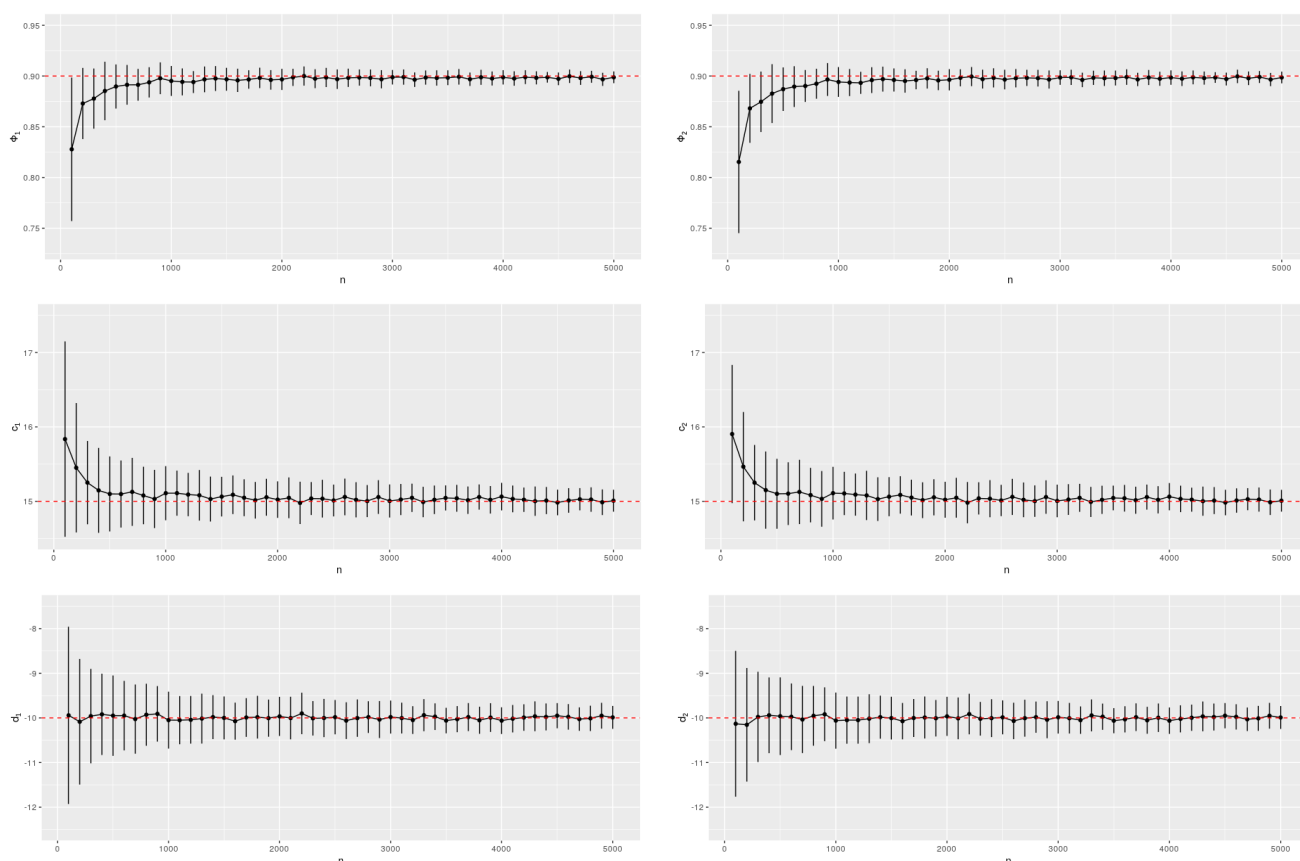


FIGURE 18. Means and standard deviation of the estimators of ϕ , c_n and d , according Theorem 2 (first column) or linear regression (second column), over 100 simulations of $(X_{n,k})_{0 \leq k \leq n}$, for $n \in \{100, 200, \dots, 5000\}$ with $\phi = 0.9$, $\nu = 0.3$, $\lambda = 1$, $c = 15$, $d = -10$, $X_0 = c_n$, with $c_n = c - d/(n(1 - \phi))$

REFERENCES

- [1] K. B. Athreya and S. G. Pantula. A note on strong mixing of ARMA processes. *Statist. Probab. Lett.*, 4(4):187–190, 1986.
- [2] K. N. Berk. A central limit theorem for m -dependent random variables with unbounded m . *Ann. Probability*, 1:352–354, 1973.
- [3] P. J. Brockwell and R. A. Davis. *Time series: theory and methods*. Springer Series in Statistics. Springer, New York, 2006. Reprint of the second (1991) edition.
- [4] B. M. Brown. Martingale central limit theorems. *Ann. Math. Statist.*, 42:59–66, 1971.
- [5] A.N. Burkitt. A review of the integrate-and-fire neuron model: I. homogeneous synaptic input. *Biological Cybernetics*, 95:1–19, 2006.
- [6] A. Caraty, P. Orgeur, and J.-C. Thierry. Demonstration of the pulsatile secretion of LH-RH into hypophysial portal blood of ewes using an original technic for multiple samples. *Comptes rendus des séances de l'Académie des sciences. Série III, Sciences de la vie*, 295:103–6, 10 1982.
- [7] I. J. Clarke and J. T. Cummins. The temporal relationship between gonadotropin releasing hormone (GnRH) and luteinizing (LH) secretion in ovariectomized ewes. *Endocrinology*, 111(5):1737–1739, 1982.
- [8] S. Constantin, A. Caraty, S. Wray, and A. Duittoz. Development of gonadotropin-releasing hormone-1 secretion in mouse nasal explants. *Endocrinology*, 150(7):3221–3227, July 2009.
- [9] P. Doukhan. *Stochastic models for time series*, volume 80 of *Mathématiques & Applications (Berlin) [Mathematics & Applications]*. Springer, Cham, 2018.
- [10] C. Fraley, A. E. Raftery, T. B. Murphy, and L. Scrucca. MCLUST Version 4 for R: Normal Mixture Modeling for Model-Based Clustering, Classification, and Density Estimation. *Technical Report No. 597*, 2012.
- [11] P. Gaenssler, J. Strobel, and W. Stute. On central limit theorems for martingale triangular arrays. *Acta Math. Acad. Sci. Hungar.*, 31(3-4):205–216, 1978.
- [12] C. Georgelin, C. Constant, H. Biermé, G. Chevrot, B. Piégu, R. Fleurot, G. Leng, and A. Duittoz. GnRH paracrine/autocrine action induced a non-stochastic behaviour andepisodic synchronisation of gnrh neurons activity: in vitro and in silico study. In preparation, 2020.

- [13] W. Gerstner and W. Kistler. *Spiking Neuron Models: An Introduction*. Cambridge University Press, New York, NY, USA, 2002.
- [14] D. M. Green and J. A. Swets. *Signal detection theory and psychophysics*. Wiley, 1966.
- [15] P. Jahn, R.W. Berg, J. Hounsgaard, and S. Ditlevsen. Motoneuron membrane potentials follow a time inhomogeneous jump diffusion process. *J. of Comput. Neurosci.*, 31:563–579, 2011.
- [16] C. F. Jeff Wu. On the convergence properties of the EM algorithm. *Ann. Statist.*, 11(1):95–103, 03 1983.
- [17] J. E. Levine, K. Y. Pau, V. D. Ramirez, and G. L. Jackson. Simultaneous measurement of luteinizing hormone-releasing hormone and luteinizing hormone release in unanesthetized, ovariectomized sheep. *Endocrinology*, 111(5):1449–1455, 1982.
- [18] N. A. Macmillan and C. D. Creelman. *Detection Theory: A User's Guide*. Psychology Press. Taylor & Francis, 2004. Reprint of the second (1991) edition.
- [19] G. McLachlan and D. Peel. *Finite Mixture Models*. Wiley Series in Probability and Statistics. Wiley, 2000.
- [20] S. M. Moenter. GnRH neuron electrophysiology: A decade of study. *Brain Research*, 1364:10–24, October 2010.
- [21] S. K. Ng, T. Krishnan, and G. J. McLachlan. *The EM algorithm*. Springer Handb. Comput. Stat. Springer, Heidelberg, 2012.
- [22] P. Perron and T. Yabu. Testing for trend in the presence of autoregressive error: a comment. *J. Amer. Statist. Assoc.*, 107(498):844, 2012.
- [23] D. Qiu, Q. Shao, and L. Yang. Efficient inference for autoregressive coefficients in the presence of trends. *J. Multivariate Anal.*, 114:40–53, 2013.
- [24] A. Roy, B. Falk, and W. A. Fuller. Testing for trend in the presence of autoregressive error. *J. Amer. Statist. Assoc.*, 99(468):1082–1091, 2004.
- [25] A. W. van der Vaart. *Asymptotic statistics*, volume 3 of *Cambridge Series in Statistical and Probabilistic Mathematics*. Cambridge University Press, Cambridge, 1998.
- [26] S. Wray. From nose to brain: development of gonadotrophin-releasing hormone-1 neurones. *Journal of neuroendocrinology*, 22(7):743–753, July 2010.

HERMINE BIERMÉ AND CAMILLE CONSTANT, LMA UMR CNRS 7348, UNIVERSITÉ DE POITIERS, BÂT. H3 - SITE DU FUTUROSCOPE, TSA 61125, 11 BD MARIE ET PIERRE CURIE, 86073 POITIERS CEDEX 9, FRANCE

E-mail address: `hermine.bierme@math.univ-poitiers.fr`, `camille.constant@math.univ-poitiers.fr`

ANNE DUITTOZ, INRA, UMR85 PHYSIOLOGIE DE LA REPRODUCTION ET DES COMPORTEMENTS, CNRS, UMR7247, IFCE, 37380 NOUZILLY, UNIVERSITÉ DE TOURS, 37000 TOURS, FRANCE

E-mail address: `anne.duittoz@univ-tours.fr`

CHRISTINE GEORGELIN, IDP UMR CNRS 7013, UNIVERSITÉ DE TOURS, UNIVERSITÉ D'ORLÉANS, PARC DE GRANDMONT 37200 TOURS, FRANCE

E-mail address: `christine.georgelin@lmpt.univ-tours.fr`